Contents

Chapter 1

Electrons in Solids

1.1 Introduction

What is the world made of? To a philosopher, this question lies at the intersection of ontology (the ‘study’ of being and existence) and mereology (the ‘study’ of parts and wholes). To a physicist, the answer very much depends on whom you ask, because ultimately it is a matter of energy scales. To a condensed matter physicist, the world consists of electrons, nuclei, and photons. That’s pretty much it[1]. The characteristic energy scales in condensed matter typically range from milli-electron volts (meV) to electron volts (eV)[2]. By contrast, the protons and neutrons which constitute nuclei typically have binding energies on the order of MeV. The nucleons themselves consist of quarks and gluons. Quarks acquire their masses from coupling to the Higgs field, but some 99% of the nucleon mass is due to gluons and virtual quark-antiquark pairs, *i.e.* to the physics of QCD binding[3].

1.1.1 Phases of matter

Condensed matter physicists are not interested in electrons, nuclei, and photons in isolation. Rather it is the collective properties of these interacting constituents which leads to the remarkably rich phenomenology of condensed matter. This richness is manifested by the bewildering array of *phases of matter* that can be conjured. Until relatively recently, phases of matter were described based on the *Landau paradigm*, in which an ordered phase is described by one or more nonzero *order parameters*, each of which describes a *broken global symmetry*. For a ferromagnet, the order parameter is the magnetization density, $\boldsymbol{m}$, and the broken symmetry is the group of rotations $\mathsf{O}(3)$ or $\mathsf{SU}(2)$, or possibly $\mathbb{Z}_2$. For a crystal or charge density wave, the order parameters are the Fourier components $\varrho_{\boldsymbol{G}}$ of the density at a series of wavevectors which comprise the reciprocal lattice of the structure. A given order parameter ϕ will in general depend on temperature T, pressure p, applied magnetic field $\boldsymbol{H}$, various coupling parameters

---

[1] Sometimes experimentalists use muons or even positrons to probe their samples, but the samples themselves consist of electrons and nuclei.

[2] Sometimes higher energy probes on the order of keV are used, for example in photoemission spectroscopy.

[3] So the next time you overhear someone holding forth about how the Higgs field (or, worse still, the Higgs boson) gives mass to everything in the universe, you can tell them that they are full of shit.

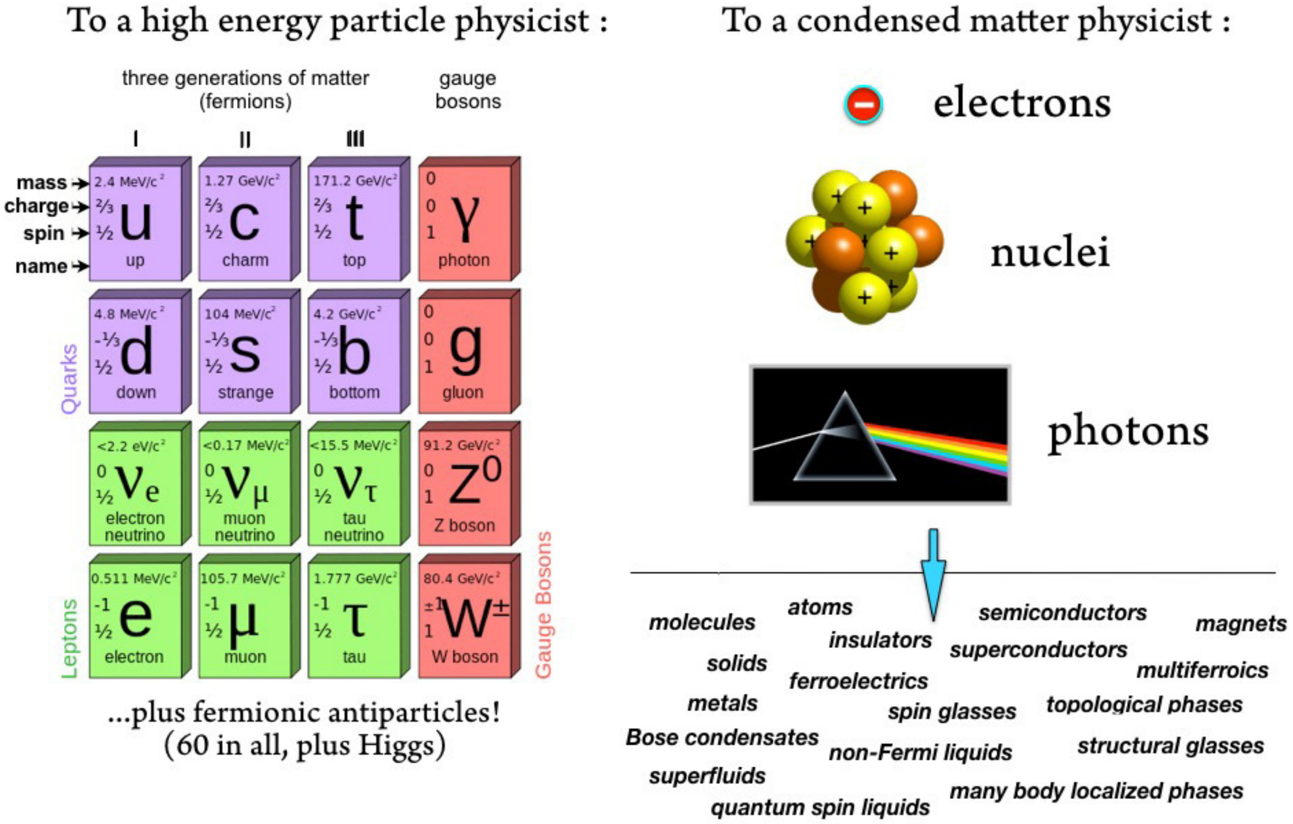

Figure 1.1: What is the world made of? It depends on whom you ask.

which enter the Hamiltonian $\{g_i\}$, *etc.* A multidimensional plot which labels the various phases of a system as a function of all these parameters is known as a *phase diagram*. Points, lines, or surfaces separating different phases are the loci of *phase transitions*, where the free energy and the order parameters of the system exhibit singularities. At a *first order transition*, certain properties change discontinuously. The parade example of a first order transition is the freezing or boiling of liquid water to solid ice or gaseous vapor. These transitions involve a discontinuous change in the density as T or p is varied so as to cross a phase boundary[4]. At a *second order transition*, one or more order parameters vanish as a phase boundary is approached. Within the Landau paradigm, a nonzero order parameter is associated with the spontaneous breaking of a symmetry, such as spin rotation (in a magnet), space translation (in a crystal), *etc.* Furthermore, a second order transition between phases A and B is possible only if the symmetry groups $G_{\rm A}$ of the A phase and $G_{\rm B}$ of the B phase, both of which must be subgroups of the symmetry group G of the Hamiltonian, satisfy $G_{\rm A} \subset G_{\rm B}$ or $G_{\rm B} \subset G_{\rm A}$. A phase transition which takes place at $T = 0$ as a function of other parameters (p, H, *etc.*) is called a *quantum phase transition*.

---

[4] The phase boundary between liquid and vapor terminates in a *critical point*, and it is therefore possible to continuously evolve from liquid to vapor without ever encountering a singularity. Thus, from the point of view of order parameters and broken symmetry, there is no essential distinction between liquid and vapor phases.

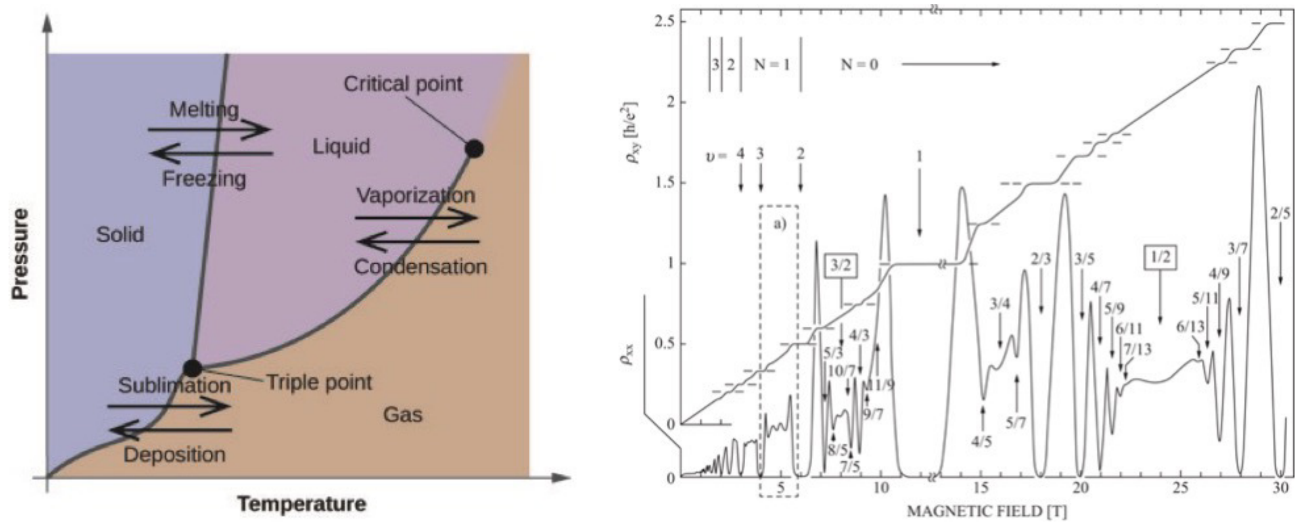

Figure 1.2: Left: Phase diagram of H_2O in the (T, p) plane. Right: Low temperature ($T \approx 150\,\mathrm{mK}$) longitudinal resistivity ρ_{xx} and Hall resistivity ρ_{xy} as a function of applied magnetic field in a two-dimensional electron gas system (GaAs/AlGaAs heterostructure), from R. Willett *et al.*, *Phys. Rev. Lett.* **59**, 1776 (1987). Each dip in ρ_{xx} and concomitant plateau in ρ_{xy} corresponds to a distinct phase of matter.

1.1.2 Beyond the Landau paradigm

Over the past 25 years or so, a new paradigm has emerged for certain phases of matter which have no order parameter in the conventional sense. These are called *topological phases*, and are exemplified by the phases of the quantum Hall effect. Typically topological phases exhibit a *bulk excitation gap*, meaning it requires a finite amount of energy in order to excite these systems in their bulk, and in this respect, they are akin to insulators. However, at the edges of finite systems, there exist *gapless edge states* which may carry current. The structure of the edge states is intimately related to the nature of the bulk phase, which despite being a condensate of sorts, has no local order parameter.

Topological phases are of intense current interest, both theoretically and experimentally, but they remain somewhat exotic, as compared with, say, metals. Yet the metallic phase, which is an example of a *Landau Fermi liquid*, is difficult to characterize in terms of a conventional order parameter[5].

Another violation of the Landau paradigm which has been revealed in recent years is the (at this point purely theoretical) notion of *deconfined quantum criticality*. A deconfined quantum critical point violated the Landau requirement that the symmetry groups on either side of the transition have a subgroup relation.

Alas, physics beyond the Landau paradigm is also beyond the scope of this course. While electronic materials, *i.e.* systems in which the essential physics is manifested in the properties of the electron degrees of freedom, do exhibit a variety of novel phases, such as the quantum Hall effect and non-Fermi liquid states, our focus shall be on "meat and potatoes" condensed matter physics of the 20^{th} century.

---

[5] The order parameter of a Fermi liquid is usually taken to be the *quasiparticle weight* Z, which, in isotropic systems, characterizes the discontinuous drop in the momentum occupation function $n(k)$ as one crosses the Fermi surface at $k = k_{\mathrm{F}}$.

הסיכום

הוגה אחד זקן
מחדרו אל תלמידיו יצא
ואמר בנקשו במקל:
שמעו אחרון דברי אשר אשא
כי הגיע הזמן לסכם,
לאחר שנות בינה ועיצה,
מה הם, לסוף מיצוי,
הדברים שמהם העולם עשוי.

העולם, נכבדי – שאחרי כל תהיות
ופליאות בו דברי אמורים –
עשוי ארץ, שמים, שיחים, סנוניות,
אוניות, גלי ים, נהרות, ערים
גדולות וקטנות, ירידים, צנוניות,
כל מיני פטישים, נייר, משורים,
רחובות, חדרים, – כך הוסיף למנות

ולמנות – גאיות, שפלות, הרים
וגבעות – ושעה שרופא ואחות
כבר עליו גחנו בבית–החולים,
עדיין היו שפתיו נעות
ומונות – קלחות, כפיות, ספרים,
מגרות, צנצנות – ומילים אחרונות
שהשמיע היו: נעצים, כפתורים.

Summary

One old thinker
out from his chamber to his disciples came
and he said as he rapped with his cane:
harken to the last of my words
for it is now time to summarize,
after years of reason and deliberation,
what, in the last analysis,
are the things of which the world is made.

The world, my distinguished sirs – which after all wondering
and marveling my words concern –
is made of land, sky, bushes, sparrows,
ships, waves, rivers, cities
large and small, fairs, radishes,
all kinds of hammers, paper, saws,
streets, rooms - thus he continued counting

and counting – valleys, plains, mountains,
hills – and while the doctor and nurse
were bent over him in the hospital,
still his lips were moving
and counting – cauldrons, spoons, books,
drawers, jars – and the last words
which he uttered were: thumbtacks, buttons.

Natan Alterman
(1910 - 1970)

(translation by Assa Auerbach)

Figure 1.3: What is the world made of? Another point of view.

1.1.3 Experimental probes

In this course we will study four important phases of condensed matter in the solid state: metals, insulators, magnets, and superconductors[6]. These phases are revealed through various experimental probes, such as specific heat, magnetic susceptibility, electrical transport (*e.g.*, resistivity), scattering (by electrons, neutrons, or photons), *etc.* The theoretical understanding of such probes typically involves the computation of correlation (or, equivalently, response) functions within the framework of quantum statistical physics.

When falsifiable theoretical models and their solutions are in harmonious agreement with experiment, and predict new observable phenomena, we can feel confident that we are indeed beginning to understand what the world is made of.

---

[6] As we shall see, semiconductors form a sub-class of insulators.

1.2 Energy Bands in Solids

1.2.1 Bloch's theorem

The Hamiltonian for an electron in a crystal is

$$H = -\frac{\hbar^2}{2m}\,\boldsymbol{\nabla}^2 + V(\boldsymbol{r}) \quad , \tag{1.1}$$

where $V(\boldsymbol{r}) = V(\boldsymbol{r}+\boldsymbol{R})$ for all $\boldsymbol{R} \in \mathcal{L}$, where $\mathcal{L}$ is the direct Bravais lattice underlying the crystal structure. The potential $V(\boldsymbol{r})$ describes the crystalline potential due to the ions, plus the average (Hartree) potential of the other electrons. The lattice translation operator is $t(\boldsymbol{R}) = \exp(i\boldsymbol{R}\cdot\boldsymbol{p}/\hbar) = \exp(\boldsymbol{R}\cdot\boldsymbol{\nabla})$. Acting on any function of $\boldsymbol{r}$, we have

$$t(\boldsymbol{R})\, f(\boldsymbol{r}) = f(\boldsymbol{r}+\boldsymbol{R}) \quad . \tag{1.2}$$

Note that lattice translations are unitary, *i.e.* $t^\dagger(\boldsymbol{R}) = t^{-1}(\boldsymbol{R}) = t(-\boldsymbol{R})$, and they satisfy the composition rule $t(\boldsymbol{R}_1)\, t(\boldsymbol{R}_2) = t(\boldsymbol{R}_1 + \boldsymbol{R}_2)$. Since $\big[t(\boldsymbol{R}), H\big] = 0$ for all Bravais lattice vectors $\boldsymbol{R}$, the Hamiltonian H and all lattice translations $t(\boldsymbol{R})$ may be simultaneously diagonalized. Let $\psi(\boldsymbol{r})$ be such a common eigenfunction. Since $t(\boldsymbol{R})$ is unitary, its eigenvalue must be a phase $\exp(i\theta_{\boldsymbol{R}})$, and as a consequence of the composition rule, we must have $\theta_{\boldsymbol{R}_1+\boldsymbol{R}_2} = \theta_{\boldsymbol{R}_1} + \theta_{\boldsymbol{R}_2}$. This requires that $\theta_{\boldsymbol{R}}$ be linear in each of the components of $\boldsymbol{R}$, *i.e.* $\theta_{\boldsymbol{R}} = \boldsymbol{k}\cdot\boldsymbol{R}$, where $\boldsymbol{k}$ is called the *wavevector*. Since $\exp(i\,\boldsymbol{G}\cdot\boldsymbol{R}) = 1$ for any $\boldsymbol{G} \in \hat{\mathcal{L}}$, *i.e.* for any reciprocal lattice vector (RLV) $\boldsymbol{G}$ in the reciprocal lattice $\widehat{\mathcal{L}}$, the wavevector is only defined modulo $\boldsymbol{G}$, which means that $\boldsymbol{k}$ may be restricted to the first Brillouin zone of the reciprocal lattice. The quantity $\hbar\boldsymbol{k}$ is called the *crystal momentum*. Unlike the ordinary momentum $\boldsymbol{p}$, crystal momentum is only conserved modulo $\hbar\boldsymbol{G}$.

The energy E will in general depend on $\boldsymbol{k}$, but there may be several distinct energy eigenstates with the same value of $\boldsymbol{k}$. We label these different energy states by a discrete index n, called the *band index*. Thus, eigenstates of H are labeled by the pair $(n,\boldsymbol{k})$, with

$$H\,\psi_{n\boldsymbol{k}}(\boldsymbol{r}) = E_n(\boldsymbol{k})\,\psi_{n\boldsymbol{k}}(\boldsymbol{r}) \qquad , \qquad t(\boldsymbol{R})\,\psi_{n\boldsymbol{k}}(\boldsymbol{r}) = e^{i\boldsymbol{k}\cdot\boldsymbol{R}}\,\psi_{n\boldsymbol{k}}(\boldsymbol{r}) \quad , \tag{1.3}$$

This is the content of *Bloch's theorem*. Note that the *cell function* $u_{n\boldsymbol{k}}(\boldsymbol{r}) \equiv \psi_{n\boldsymbol{k}}(\boldsymbol{r})\, e^{-i\boldsymbol{k}\cdot\boldsymbol{r}}$ is periodic in the direct lattice, with $u_{n\boldsymbol{k}}(\boldsymbol{r}+\boldsymbol{R}) = u_{n\boldsymbol{k}}(\boldsymbol{r})$. Thus, each Bloch function $\psi_{n\boldsymbol{k}}(\boldsymbol{r})$ may be written as the product of a plane wave and a cell function, *viz.*

$$\psi_{n\boldsymbol{k}}(\boldsymbol{r}) \equiv \langle\, \boldsymbol{r} \,|\, n\boldsymbol{k}\,\rangle = e^{i\boldsymbol{k}\cdot\boldsymbol{r}}\, u_{n\boldsymbol{k}}(\boldsymbol{r}) \quad . \tag{1.4}$$

We may always choose the Bloch functions to be periodic in the reciprocal lattice, *i.e.* $\psi_{n,\boldsymbol{k}+\boldsymbol{G}}(\boldsymbol{r}) = \psi_{\boldsymbol{k}}(\boldsymbol{r})$. This choice entails the condition $u_{n,\boldsymbol{k}+\boldsymbol{G}}(\boldsymbol{r}) = u_{n\boldsymbol{k}}(\boldsymbol{r})\, e^{-i\boldsymbol{G}\cdot\boldsymbol{r}}$. However, there is no guarantee that $\psi_{n\boldsymbol{k}}(\boldsymbol{r})$ is continuous as a function of $\boldsymbol{k} \in \mathbb{R}^d$. As an example, consider the one-dimensional Bloch function $\psi_{nk}(x) = L^{-1/2}\, e^{i(G_n+k)x}$, where n labels the reciprocal lattice vector $G_n = 2\pi n/a$. If $\psi_{nk}(x)$ is taken to be continuous as a function of k, then clearly $\psi_{n,k+G_m}(x) = \psi_{n,k}(x)\, e^{iG_m x} = \psi_{n+m,k}(x) \neq \psi_{nk}(x)$.

The Bloch states, being eigenstates of a Hermitian operator, satisfy the conditions of completeness,

$$\sum_{n,\boldsymbol{k}} |\, n\boldsymbol{k}\,\rangle\langle\, n\boldsymbol{k}\,| = 1 \quad , \tag{1.5}$$

and orthonormality,

$$\langle\, n\boldsymbol{k} \,|\, n'\boldsymbol{k}' \,\rangle = \delta_{nn'}\, \delta_{\boldsymbol{k}\boldsymbol{k}'} \quad . \tag{1.6}$$

Here we have assumed quantization of $\boldsymbol{k}$ in a large box of dimensions $L_1 \times L_2 \times L_3$. Each allowed wavevector then takes the form $\boldsymbol{k} = \big(\frac{2\pi n_1}{L_1}, \frac{2\pi n_2}{L_2}, \frac{2\pi n_3}{L_3}\big)$, where $n_{1,2,3} \in \mathbb{Z}$. In the thermodynamic limit, where $L_{1,2,3} \to \infty$, we have

$$\sum_{\boldsymbol{k}} \longrightarrow N v_0 \int \frac{d^d\boldsymbol{k}}{(2\pi)^d} \quad , \tag{1.7}$$

where d is the dimension of space ($d = 3$ unless otherwise noted), v_0 is the unit cell volume in real space, *i.e.* the volume of the Wigner-Seitz cell, and $N = L_1 \cdots L_d / v_0$ is the number of unit cells in the system, and is assumed to be thermodynamically large. Thus, we have from Eqn. 1.5,

$$\delta(\boldsymbol{r} - \boldsymbol{r}') = N v_0 \int \frac{d^d\boldsymbol{k}}{(2\pi)^d}\, \psi_{n\boldsymbol{k}}(\boldsymbol{r})\, \psi^*_{n\boldsymbol{k}}(\boldsymbol{r}') \quad . \tag{1.8}$$

One can see how the above equation is true in the simple case where $u_{n\boldsymbol{k}}(\boldsymbol{r}) = 1$ and $\psi_{n\boldsymbol{k}}(\boldsymbol{r}) = V^{-1/2}\, e^{i\boldsymbol{k}\cdot\boldsymbol{r}}$, with $V = N v_0$.

1.2.2 Schrödinger equation

The potential $V(\boldsymbol{r})$ has a discrete Fourier representation as

$$V(\boldsymbol{r}) = \sum_{\boldsymbol{G}} V_{\boldsymbol{G}}\, e^{i\boldsymbol{G}\cdot\boldsymbol{r}} \quad , \tag{1.9}$$

where the sum is over all reciprocal lattice vectors $\boldsymbol{G} \in \hat{\mathcal{L}}$. Since $V(\boldsymbol{r})$ is a real function, we must have $V_{-\boldsymbol{G}} = V^*_{\boldsymbol{G}}$. Any Bloch function $\psi_{\boldsymbol{k}}(\boldsymbol{r})$ may also be written as a Fourier sum, *viz.*

$$\psi_{\boldsymbol{k}}(\boldsymbol{r}) = \sum_{\boldsymbol{G}} C_{\boldsymbol{G}}(\boldsymbol{k})\, e^{i(\boldsymbol{G}+\boldsymbol{k})\cdot\boldsymbol{r}} \quad . \tag{1.10}$$

If we choose the Bloch functions to be periodic in the reciprocal lattice, then $C_{\boldsymbol{G}}(\boldsymbol{k}) = C(\boldsymbol{G} + \boldsymbol{k})$ is a function of $\boldsymbol{G} + \boldsymbol{k}$. Here, we have suppressed the band index n, and the wavevector $\boldsymbol{k} \in \hat{\Omega}$ must lie within the first Brillouin zone. The Schrödinger equation $H\psi_{\boldsymbol{k}}(\boldsymbol{r}) = E(\boldsymbol{k})\, \psi_{\boldsymbol{k}}(\boldsymbol{r})$ then takes the form

$$\frac{\hbar^2(\boldsymbol{G}+\boldsymbol{k})^2}{2m}\, C_{\boldsymbol{G}}(\boldsymbol{k}) + \sum_{\boldsymbol{G}'} V_{\boldsymbol{G}-\boldsymbol{G}'}\, C_{\boldsymbol{G}'}(\boldsymbol{k}) = E(\boldsymbol{k})\, C_{\boldsymbol{G}}(\boldsymbol{k}) \quad . \tag{1.11}$$

Note that we have one such equation for each wavevector $\boldsymbol{k} \in \hat{\Omega}$. This equation can be written in matrix form, as

$$\sum_{\boldsymbol{G}'} H_{\boldsymbol{G}\boldsymbol{G}'}(\boldsymbol{k})\, C_{\boldsymbol{G}'}(\boldsymbol{k}) = E(\boldsymbol{k})\, C_{\boldsymbol{G}}(\boldsymbol{k}) \quad , \tag{1.12}$$

where, for each $\boldsymbol{k}$, $H_{\boldsymbol{G}\boldsymbol{G}'}(\boldsymbol{k})$ is an infinite rank matrix,

$$H_{\boldsymbol{G}\boldsymbol{G}'}(\boldsymbol{k}) = \frac{\hbar^2(\boldsymbol{G}+\boldsymbol{k})^2}{2m}\, \delta_{\boldsymbol{G}\boldsymbol{G}'} + V_{\boldsymbol{G}-\boldsymbol{G}'} \quad , \tag{1.13}$$

whose rows and columns are indexed by reciprocal lattice vectors $\boldsymbol{G}$ and $\boldsymbol{G}'$, respectively. The solutions, for any fixed value of $\boldsymbol{k}$, are then labeled by a band index n, hence

$$\psi_{n\boldsymbol{k}}(\boldsymbol{r}) = \overbrace{\bigg(\sum_{\boldsymbol{G}} C^{(n)}_{\boldsymbol{G}}(\boldsymbol{k})\, e^{i\boldsymbol{G}\cdot\boldsymbol{r}}\bigg)}^{\text{cell function } u_{n\boldsymbol{k}}(\boldsymbol{r})} e^{i\boldsymbol{k}\cdot\boldsymbol{r}} \quad . \tag{1.14}$$

Note how the cell function $u_{n\boldsymbol{k}}(\boldsymbol{r})$ is explicitly periodic under direct lattice translations $\boldsymbol{r} \to \boldsymbol{r} + \boldsymbol{R}$. Note also that $u_{n\boldsymbol{k}}(\boldsymbol{r})$ is an eigenfunction of the unitarily transformed Hamiltonian

$$\begin{aligned} H(\boldsymbol{k}) \equiv e^{-i\boldsymbol{k}\cdot\boldsymbol{r}}\, H\, e^{i\boldsymbol{k}\cdot\boldsymbol{r}} &= \frac{(\boldsymbol{p} + \hbar\boldsymbol{k})^2}{2m} + V(\boldsymbol{r}) \\ H(\boldsymbol{k})\, u_{n\boldsymbol{k}}(\boldsymbol{r}) &= E_n(\boldsymbol{k})\, u_{n\boldsymbol{k}}(\boldsymbol{r}) \quad . \end{aligned} \tag{1.15}$$

1.2.3 $V = 0$: empty lattice

Consider the case of $d = 1$ with $V = 0$, *i.e.* an empty lattice. We can read off the eigenvalues of $H_{GG'}$ from Eqn. 1.13: $E_{nk} = \hbar^2(G + k)^2/2m$, where the band index n identifies the reciprocal lattice vector $G = 2\pi n/a$, where a is the lattice spacing[7]. The first Brillouin zone $\hat{\Omega}$ is the region $k \in \big[-\frac{\pi}{a}\,,\,\frac{\pi}{a}\big]$. Fig. 1.4 shows how the usual ballistic dispersion $E(q) = \hbar^2 q^2/2m$ is "folded" into the first Brillouin zone by translating sections by integer multiples of the primary reciprocal lattice vector $b \equiv 2\pi/a$.

1.2.4 Perturbation theory

Let's consider the case where the potential $V(\boldsymbol{r})$ is weak. This is known as the *nearly free electron* (NFE) model. The matrix form of the Hamiltonian $H_{\boldsymbol{G}\boldsymbol{G}'}(\boldsymbol{k})$ is given by

$$H_{\boldsymbol{G}\boldsymbol{G}'}(\boldsymbol{k}) = \begin{pmatrix} \frac{\hbar^2(\boldsymbol{G}_1+\boldsymbol{k})^2}{2m} + V_0 & V_{\boldsymbol{G}_1-\boldsymbol{G}_2} & V_{\boldsymbol{G}_1-\boldsymbol{G}_3} & \cdots \\ V^*_{\boldsymbol{G}_1-\boldsymbol{G}_2} & \frac{\hbar^2(\boldsymbol{G}_2+\boldsymbol{k})^2}{2m} + V_0 & V_{\boldsymbol{G}_2-\boldsymbol{G}_3} & \cdots \\ V^*_{\boldsymbol{G}_1-\boldsymbol{G}_3} & V^*_{\boldsymbol{G}_2-\boldsymbol{G}_3} & \frac{\hbar^2(\boldsymbol{G}_3+\boldsymbol{k})^2}{2m} + V_0 & \cdots \\ \vdots & \vdots & \vdots & \ddots \end{pmatrix} \quad . \tag{1.16}$$

Suppose we perturb in the off-diagonal elements, going to second order in $V_{\boldsymbol{G}-\boldsymbol{G}'}$. We then obtain

$$E_{\boldsymbol{G}}(\boldsymbol{k}) = E^0_{\boldsymbol{G}}(\boldsymbol{k}) + V_0 + \sum_{\boldsymbol{G}'(\neq \boldsymbol{G})} \frac{\big|V_{\boldsymbol{G}-\boldsymbol{G}'}\big|^2}{E^0_{\boldsymbol{G}}(\boldsymbol{k}) - E^0_{\boldsymbol{G}'}(\boldsymbol{k})} + \mathcal{O}(V^3) \quad , \tag{1.17}$$

---

[7] Since the lattice is empty, we can use any value for a we please. The eigenspectrum will be identical, although the labeling of the eigenstates will depend on a since this defines the size of the Brillouin zone.

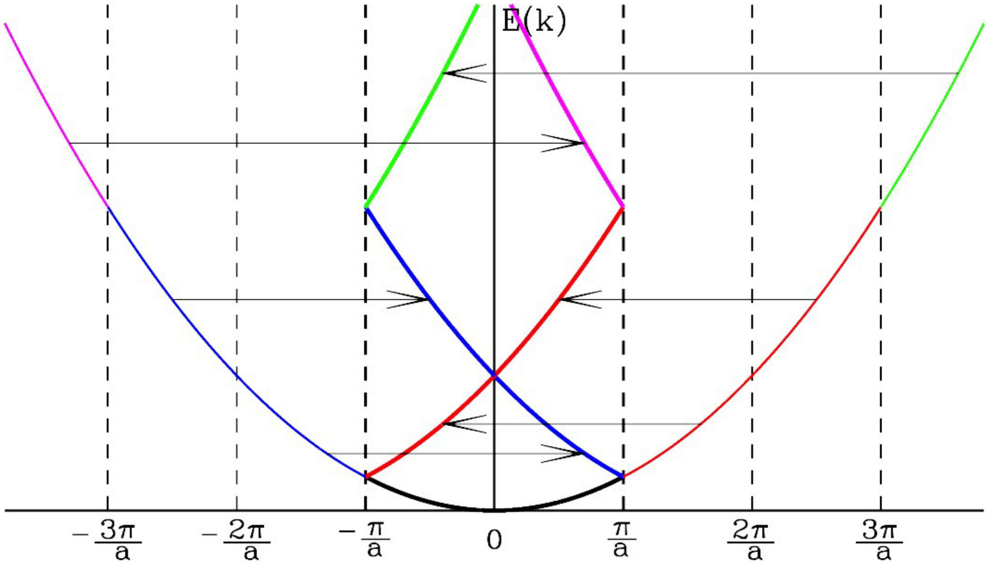

Figure 1.4: Band structure for an empty one-dimensional lattice, showing how the quadratic dispersion is "folded" from the extended zone picture into the first Brillouin zone.

where the unperturbed eigenvalues are $E^0_{\boldsymbol{G}}(\boldsymbol{k}) = \hbar^2(\boldsymbol{G}+\boldsymbol{k})^2/2m$. Note that the term with $\boldsymbol{G}' = \boldsymbol{G}$ is excluded from the sum. Here and henceforth, we shall set $V_0 \equiv 0$. The denominator in the above sum can vanish if a $\boldsymbol{G}'$ can be found such that $E^0_{\boldsymbol{G}}(\boldsymbol{k}) = E^0_{\boldsymbol{G}'}(\boldsymbol{k})$. In this case, the calculation fails, and we must use degenerate perturbation theory.

Zone center (Γ), $\boldsymbol{G} = 0$

Let's first look in the vicinity of the zone center, labeled Γ, *i.e.* $\boldsymbol{k} \approx 0$. For the band associated with $\boldsymbol{G} = 0$, we have

$$\begin{aligned} E_0(\boldsymbol{k}) &= \frac{\hbar^2\boldsymbol{k}^2}{2m} - \frac{2m}{\hbar^2}\sum_{\boldsymbol{G}(\neq 0)} \frac{|V_{\boldsymbol{G}}|^2}{\boldsymbol{G}^2 + 2\boldsymbol{G}\cdot\boldsymbol{k}} + \mathcal{O}(V^3) \\ &= \frac{\hbar^2\boldsymbol{k}^2}{2m} - \frac{2m}{\hbar^2}\sum_{\boldsymbol{G}(\neq 0)} \frac{|V_{\boldsymbol{G}}|^2}{|\boldsymbol{G}|^2}\left\{1 - \frac{2\,\boldsymbol{G}\cdot\boldsymbol{k}}{|\boldsymbol{G}|^2} + \frac{4(\boldsymbol{G}\cdot\boldsymbol{k})^2}{|\boldsymbol{G}|^4} + \ldots\right\} + \mathcal{O}(V^3) \quad . \end{aligned} \tag{1.18}$$

Since $V_{-\boldsymbol{G}} = V^*_{\boldsymbol{G}}$, the second term inside the curly bracket vanishes upon summation, so we have

$$E_0(\boldsymbol{k}) = \varDelta + \tfrac{1}{2}\hbar^2(m^*)^{-1}_{\mu\nu}\,k^\mu\,k^\nu + \ldots \quad , \tag{1.19}$$

where

$$\begin{aligned} \varDelta &= -\frac{2m}{\hbar^2}\sum_{\boldsymbol{G}(\neq 0)} \frac{|V_{\boldsymbol{G}}|^2}{|\boldsymbol{G}|^2} \\ (m^*)^{-1}_{\mu\nu} &= \frac{1}{m}\,\delta_{\mu\nu} - \left(\frac{4\sqrt{m}}{\hbar^2}\right)^2 \sum_{\boldsymbol{G}(\neq 0)} \frac{|V_{\boldsymbol{G}}|^2}{|\boldsymbol{G}|^6}\,G^\mu\,G^\nu + \ldots \quad . \end{aligned} \tag{1.20}$$

Here $\varDelta$ is the *band offset* relative to the unperturbed case, and $(m^*)^{-1}_{\mu\nu}$ are the components of the inverse *effective mass tensor*. Note that the dispersion in general is no longer isotropic. Rather, the effective mass tensor $m^*_{\mu\nu}$ transforms according to a tensor representation of the crystallographic point group. For three-dimensional systems with cubic symmetry, m^* is a multiple of the identity, for the same reason that the inertia tensor of a cube is $I = \frac{1}{6}Ma^2\,\mathsf{diag}(1,1,1)$. But for a crystal with a tetragonal symmetry, in which one of the cubic axes is shortened or lengthened, the effective mass tensor along principal axes takes the general form $m^* = \mathsf{diag}(m_x, m_x, m_z)$, with $m_x \neq m_z$ in general.

Zone center (Γ), $\boldsymbol{G} = \pm\boldsymbol{b}_{1,2,3}$

Consider the cubic lattice with primitive direct lattice vectors $\boldsymbol{a}_j = a\,\hat{\mathbf{e}}_j$ and primitive reciprocal lattice vectors $\boldsymbol{b}_j = \frac{2\pi}{a}\,\hat{\mathbf{e}}_j$. For $\boldsymbol{k} = 0$, the six bands corresponding to $\boldsymbol{G} = \pm\boldsymbol{b}_j$ with $j \in \{1,2,3\}$ are degenerate, with $E^0_{\boldsymbol{G}} = 2\pi^2\hbar^2/ma^2$. Focusing only on these rows and columns, we obtain a 6×6 effective Hamiltonian,

$$H_{6\times6} = \begin{pmatrix} \frac{\hbar^2}{2m}\,(\boldsymbol{b}_1+\boldsymbol{k})^2 & V_{2\boldsymbol{b}_1} & V_{\boldsymbol{b}_1-\boldsymbol{b}_2} & V_{\boldsymbol{b}_1+\boldsymbol{b}_2} & V_{\boldsymbol{b}_1-\boldsymbol{b}_3} & V_{\boldsymbol{b}_1+\boldsymbol{b}_3} \\ V^*_{2\boldsymbol{b}_1} & \frac{\hbar^2}{2m}\,(\boldsymbol{b}_1-\boldsymbol{k})^2 & V^*_{\boldsymbol{b}_1+\boldsymbol{b}_2} & V^*_{\boldsymbol{b}_1-\boldsymbol{b}_2} & V^*_{\boldsymbol{b}_1+\boldsymbol{b}_3} & V^*_{\boldsymbol{b}_1-\boldsymbol{b}_3} \\ V^*_{\boldsymbol{b}_1-\boldsymbol{b}_2} & V_{\boldsymbol{b}_1+\boldsymbol{b}_2} & \frac{\hbar^2}{2m}\,(\boldsymbol{b}_2+\boldsymbol{k})^2 & V_{2\boldsymbol{b}_2} & V_{\boldsymbol{b}_2-\boldsymbol{b}_3} & V_{\boldsymbol{b}_2+\boldsymbol{b}_3} \\ V^*_{\boldsymbol{b}_1+\boldsymbol{b}_2} & V_{\boldsymbol{b}_1-\boldsymbol{b}_2} & V^*_{2\boldsymbol{b}_2} & \frac{\hbar^2}{2m}\,(\boldsymbol{b}_2-\boldsymbol{k})^2 & V^*_{\boldsymbol{b}_2+\boldsymbol{b}_3} & V^*_{\boldsymbol{b}_2-\boldsymbol{b}_3} \\ V^*_{\boldsymbol{b}_1-\boldsymbol{b}_3} & V_{\boldsymbol{b}_1+\boldsymbol{b}_3} & V^*_{\boldsymbol{b}_2-\boldsymbol{b}_3} & V_{\boldsymbol{b}_2+\boldsymbol{b}_3} & \frac{\hbar^2}{2m}\,(\boldsymbol{b}_3+\boldsymbol{k})^2 & V_{2\boldsymbol{b}_3} \\ V^*_{\boldsymbol{b}_1+\boldsymbol{b}_3} & V_{\boldsymbol{b}_1-\boldsymbol{b}_3} & V^*_{\boldsymbol{b}_2+\boldsymbol{b}_3} & V_{\boldsymbol{b}_2-\boldsymbol{b}_3} & V^*_{2\boldsymbol{b}_3} & \frac{\hbar^2}{2m}\,(\boldsymbol{b}_3-\boldsymbol{k})^2 \end{pmatrix} . \tag{1.21}$$

To simplify matters, suppose that the only significant Fourier components $V_{\boldsymbol{G}}$ are those with $\boldsymbol{G} = \pm 2\boldsymbol{b}_j$. In this case, the above 6×6 matrix becomes block diagonal, *i.e.* a direct sum of 2×2 blocks, each of which resembles

$$H_{2\times2}(\Gamma) = \begin{pmatrix} \frac{\hbar^2}{2m}(\boldsymbol{b}_j+\boldsymbol{k})^2 & V_{2\boldsymbol{b}_j} \\ V^*_{2\boldsymbol{b}_j} & \frac{\hbar^2}{2m}(\boldsymbol{b}_j-\boldsymbol{k})^2 \end{pmatrix} . \tag{1.22}$$

Diagonalizing, we obtain

$$E_{j,\pm}(\boldsymbol{k}) = \frac{\hbar^2\boldsymbol{b}_j^2}{2m} + \frac{\hbar^2\boldsymbol{k}^2}{2m} \pm \sqrt{\left(\frac{\hbar^2}{m}\,\boldsymbol{b}_j\cdot\boldsymbol{k}\right)^2 + |V_{2\boldsymbol{b}_j}|^2} . \tag{1.23}$$

Assuming cubic symmetry with $V_{\boldsymbol{b}_1} = V_{\boldsymbol{b}_2} = V_{\boldsymbol{b}_3} = V$, we obtain six bands,

$$E_{j,\pm}(\boldsymbol{k}) = \frac{2\pi^2\hbar^2}{ma^2} + \frac{\hbar^2\boldsymbol{k}^2}{2m} \pm \sqrt{\left(\frac{2\pi\hbar^2}{ma}\,k_j\right)^2 + |V|^2} . \tag{1.24}$$

The band gap at $\boldsymbol{k} = 0$ is then $2\,|V|$.

Zone edge (X), $\boldsymbol{G}=0$

Consider now the case $\boldsymbol{k}=\frac{1}{2}\boldsymbol{b}+\boldsymbol{q}$ with $|\boldsymbol{q}a|\ll 1$, and the band $\boldsymbol{G}=0$. This state is nearly degenerate with one in the band with $\boldsymbol{G}=-\boldsymbol{b}$. Isolating these contributions to $H_{\boldsymbol{G}\boldsymbol{G}'}$, we obtain the 2×2 matrix

$$H_{2\times 2}(\mathrm{X})=\begin{pmatrix}\frac{\hbar^2}{2m}\big(\frac{1}{2}\boldsymbol{b}+\boldsymbol{q}\big)^2 & V_{-\boldsymbol{b}} \\ V_{\boldsymbol{b}} & \frac{\hbar^2}{2m}\big(-\frac{1}{2}\boldsymbol{b}+\boldsymbol{q}\big)^2\end{pmatrix}\quad , \tag{1.25}$$

with dispersion

$$E_{\pm}(\boldsymbol{k})=\frac{\hbar^2\boldsymbol{b}^2}{8m}+\frac{\hbar^2\boldsymbol{q}^2}{2m}\pm\sqrt{\left(\frac{\hbar^2}{2m}\,\boldsymbol{b}\cdot\boldsymbol{q}\right)^2+|V_{\boldsymbol{b}}|^2}\quad . \tag{1.26}$$

The band gap is again $2\,|V_{\boldsymbol{b}}|$.

1.2.5 Solvable model : one-dimensional Dirac comb

Consider the one-dimensional periodic potential,

$$V(x)=-W_0\sum_{n=-\infty}^{\infty}\delta(x-na) \tag{1.27}$$

with $W_0>0$. Define $W_0\equiv\hbar^2/2m\sigma$, where σ is the *scattering length*. The Hamiltonian is then

$$H=-\frac{\hbar^2}{2m}\frac{\partial^2}{\partial x^2}-\frac{\hbar^2}{2m\sigma}\sum_n\delta(x-na)\quad . \tag{1.28}$$

The eigenstates of H must satisfy Bloch's theorem: $\psi_{nk}(x+a)=e^{ika}\,\psi_{nk}(x)$. Thus, we may write

$$\begin{aligned} x\in[-a\,,\,0] \quad &: \quad \psi_{nk}(x)=A\,e^{iqx}+B\,e^{-iqx} \\ x\in[0\,,\,+a] \quad &: \quad \psi_{nk}(x)=e^{ika}\,\psi_{nk}(x-a) \\ &\qquad\qquad\;\, =A\,e^{i(k-q)a}\,e^{iqx}+B\,e^{i(k+q)a}\,e^{-iqx}\quad . \end{aligned} \tag{1.29}$$

Continuity at $x=0$ requires $\psi_{nk}(0^-)=\psi_{nk}(0^+)$, or

$$A+B=A\,e^{i(k-q)a}+B\,e^{i(k+q)a}\quad . \tag{1.30}$$

A second equation follows from integrating the Schrödinger equation from $x=0^-$ to $x=0^+$:

$$\begin{aligned}\int\limits_{0^-}^{0^+}\!dx\;H\,\psi_{nk}(x)&=\int\limits_{0^-}^{0^+}\!dx\left\{-\frac{\hbar^2}{2m}\frac{d^2\psi_{nk}}{dx^2}-\frac{\hbar^2}{2m\sigma}\,\psi_{nk}(x)\,\delta(x)\right\} \\ &=\frac{\hbar^2}{2m}\Big[\psi'_{nk}(0^-)-\psi'_{nk}(0^+)\Big]-\frac{\hbar^2}{2m\sigma}\,\psi_{nk}(0)\quad .\end{aligned} \tag{1.31}$$

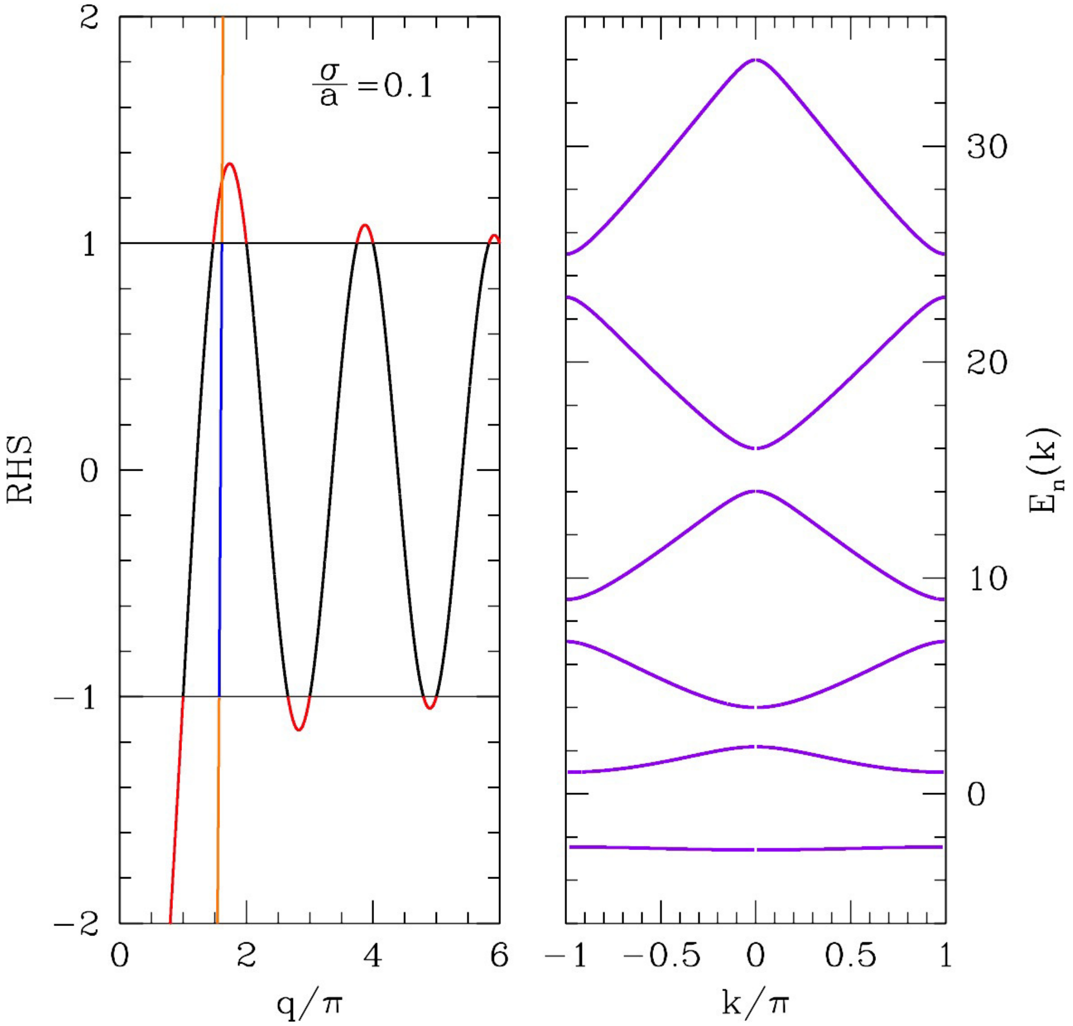

Figure 1.5: Left: Plots of the RHS of Eqns. 1.35 (black and red) and 1.36 (blue and orange) for the Dirac comb potential with scattering length $\sigma = 0.1\,a$. Allowed solutions (black and blue portions) must satisfy RHS $\in [-1,1]$. Right: Corresponding energy band structure.

Since $H\psi_{nk}(x) = E_n(k)\psi_{nk}(x)$, the LHS of the above equation is infinitesimal. Thus,

$$\psi'_{nk}(0^-) - \psi'_{nk}(0^+) = \frac{1}{\sigma}\,\psi_{nk}(0) \quad , \tag{1.32}$$

or

$$A - B - A\,e^{i(k-q)a} + Be^{i(k+q)a} = \frac{A+B}{iq\sigma} \quad . \tag{1.33}$$

The two independent equations we have derived can be combined in the form

$$\begin{pmatrix} e^{i(k-q)a} - 1 & e^{i(k+q)a} - 1 \\ e^{i(k-q)a} - 1 - \frac{i}{q\sigma} & 1 - e^{i(k+q)a} - \frac{i}{q\sigma} \end{pmatrix} \begin{pmatrix} A \\ B \end{pmatrix} = 0 \quad . \tag{1.34}$$

In order that the solution be nontrivial, we set the determinant to zero, which yields the condition

$$\cos(ka) = \cos(qa) - \frac{a}{2\sigma} \cdot \frac{\sin(qa)}{qa} \quad . \tag{1.35}$$

This is to be regarded as an equation for $q(k)$, parameterized by the dimensionless quantity σ/a. The energy eigenvalue is $E_n(k) = \hbar^2 q^2/2m$. If we set $q \equiv iQ$, the above equation becomes

$$\cos(ka) = \cosh(Qa) - \frac{a}{2\sigma} \cdot \frac{\sinh(Qa)}{Qa} \quad . \tag{1.36}$$

Here we solve for $Q(k)$, and the energy eigenvalue is $E_n(k) = -\hbar^2 Q^2/2m$. In each case, there is a discrete infinity of solutions indexed by the band index n. Results for the case $\sigma = 0.1\,a$ are shown in Fig. 1.5. In the limit $\sigma \to 0$, the solutions to Eqn. 1.35 are $q = k + \frac{2\pi n}{a}$, and we recover the free electron bands in the reduced zone scheme. When $\sigma = 0$, the only solution to Eqn. 1.36 is $Q = 0$ for the case $k = 0$.

As $q \to \infty$, the second term on the RHS of Eqn. 1.35 becomes small, and the solution for the n^{th} band ($n \in \mathbb{Z}_+$) tends to $q = k + 2\pi n/a$. The band gaps at $k = 0$ and $k = \pi$ become smaller and smaller with increasing band index. Clearly Eqn. 1.36 has no solutions for sufficiently large Q, since the RHS increases exponentially. Note that there is one band in the right panel of Fig. 1.5 with negative energy. This is because we have taken the potential $V(x)$ to be attractive. Recall that the potential $V(x) = -W_0\,\delta(x)$ has a single bound state $\psi_0(x) = \frac{1}{2\sqrt{\sigma}}\, e^{-|x|/2\sigma}$, again with $\sigma \equiv \hbar^2/2mW_0$. For the Dirac comb, the bound states in different unit cells overlap, which leads to dispersion. If $W_0 < 0$, the potential is purely repulsive, and all energy eigenvalues are positive. (There is no solution to Eqn. 1.36 when $\sigma < 0$.)

1.2.6 Diamond lattice bands

In dimensions $d > 1$, the essential physics is similar to what was discussed in the case of the NFE model, but the labeling of the bands and the wavevectors is more complicated than in the $d = 1$ case. Consider

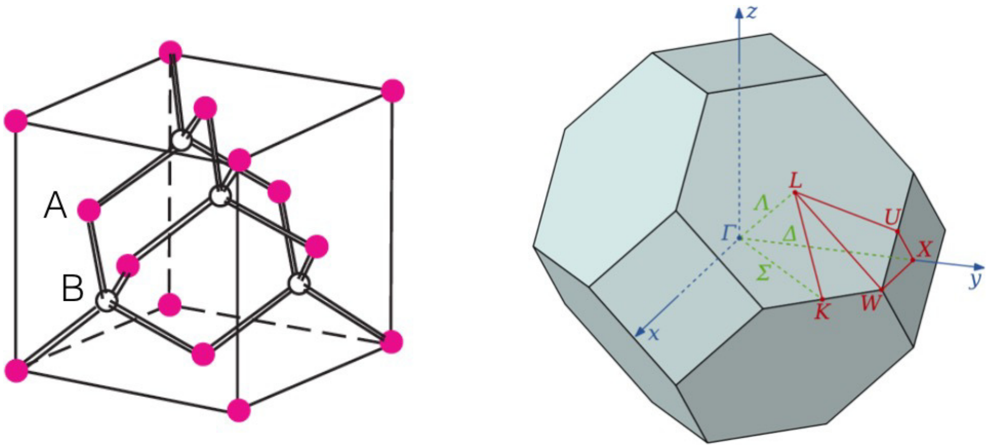

Figure 1.6: Left: The zincblende structure consists of two interpenetrating fcc lattices. Right: First Brillouin zone for the fcc lattice, with high symmetry points identified. From Wikipedia.

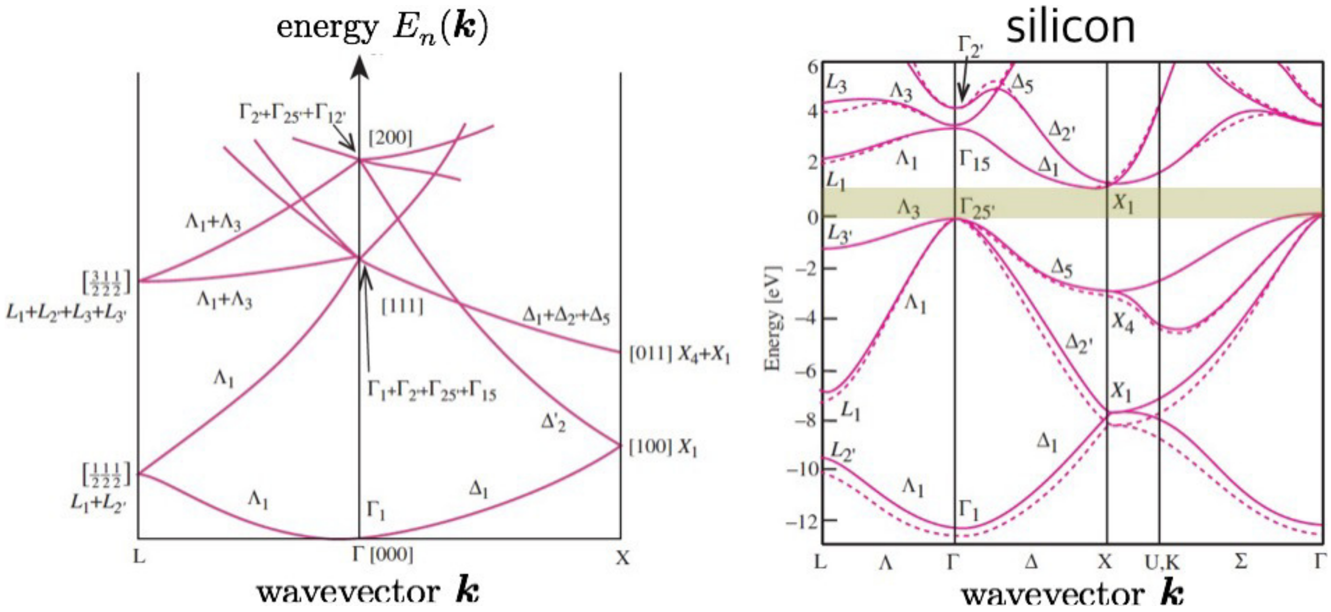

Figure 1.7: Left: Empty lattice bands for the diamond structure. Right: Electronic band structure of Si based on local (dashed) and nonlocal (solid) pseudopotential calculations. The shaded region contains no electronic eigenstates, and reflects a (indirect) *band gap*. From ch. 2 of P. Yu and M. Cardona, *Fundamentals of Semiconductors* (Springer, 1996).

the zincblende structure depicted in the left panel of Fig. 1.6. Zincblende consists of two interpenetrating face centered cubic lattices (labeled A and B in the figure), and is commonly found in nature (*e.g.*, in GaAs, InP, ZnTe, ZnS, HgTe, CdTe, *etc.*). Diamond is a homonuclear form of zincblende in which the ions on the two fcc sublattices are identical; the most familiar examples are C (carbon diamond) and Si. For both zincblende and diamond, the underlying Bravais lattice is fcc; the first Brillouin zone of the fcc lattice is depicted in the right panel of Fig. 1.6.

The left panel of Fig. 1.7 depicts the empty lattice (free electron) energy bands for the diamond structure along linear segments LΓ and ΓX (see Fig. 1.6 for the letter labels of high symmetry points). Energy levels at high symmetry points are labeled by reciprocal lattice vectors (square brackets) in the extended zone scheme, all in units of $2\pi/a$, where a is the size of the unit cube in Fig. 1.6. The other labels denote group representations under which the electronic eigenstates transform. In the extended zone scheme, the dispersion is $E(\boldsymbol{k}) = \hbar^2\boldsymbol{k}^2/2m$, so all the branches of the dispersion in the reduced zone scheme correspond to displacements of sections of this paraboloid by RLVs.

The right panel of Fig. 1.7 depicts the energy bands of crystalline silicon (Si), which has the diamond lattice structure. Notice how the lowest L-point energy levels are no longer degenerate. A gap has opened, as we saw in our analysis of the NFE model. Indeed, between $E = 0$ and $E = 1.12\,\text{eV}$, there are *no* electronic energy eigenstates. This is the 'band gap' of silicon. Note that the $1.12\,\text{eV}$ gap is *indirect* – it is between states at the Γ and X points. If the minimum energy gap occurs between levels at the same wavevector, the gap is said to be *direct*. In intrinsic semiconductors and insulators, *transport* measurements typically can provide information on indirect gaps. *Optical* measurements, however, reveal direct gaps. The reason is that the speed of light is very large, and momentum conservation

material	gap (eV)	type	material	gap	type	material	gap	type
C	5.47	indirect	Si	1.14	indirect	h-BN	5.96	direct
Ge	0.67	indirect	Sn	$\lesssim 0.08$	indirect	AlN	6.28	direct
GaN	3.44	direct	InN	0.7	direct	ZnO	3.37	direct
GaAs	1.43	direct	InP	1.35	direct	ZnSe	2.7	direct
GaP	2.26	indirect	InAs	0.36	direct	ZnS	3.54	direct
GaSb	0.726	direct	InSb	0.17	direct	ZnTe	2.25	direct
CdS	2.42	direct	CdTe	1.49	direct	Cu_2S	1.2	indirect

Table 1.1: Common semiconductors and their band gaps.

requires optical transitions to be essentially vertical in $(\boldsymbol{k}, E)$ space.

1.3 Metals and Insulators

1.3.1 Density of states

In addition to energy eigenstates being labeled by band index ν and (crystal) wavevector $\boldsymbol{k}$, they are also labeled by spin polarization $\sigma = \pm 1$ relative to some fixed axis in internal space (typically $\hat{\boldsymbol{z}}$)[8]. The component of the spin angular momentum along $\hat{\boldsymbol{z}}$ is then $S^z = \frac{1}{2}\hbar\sigma = \pm\frac{1}{2}\hbar$. Typically, $E_\nu(\boldsymbol{k},\sigma)$ is independent of the spin polarization σ, but there are many examples where this is not the case[9].

The *density of states* (DOS) per unit energy per unit volume, $g(\varepsilon)$, is given by

$$g(\varepsilon) = \frac{1}{V}\sum_{\nu,\boldsymbol{k},\sigma}{}' \delta\big(\varepsilon - E_\nu(\boldsymbol{k},\sigma)\big) \overset{V\to\infty}{=} \sum_\nu \sum_\sigma \int\limits_{\hat{\Omega}} \frac{d^dk}{(2\pi)^d}\, \delta\big(\varepsilon - E_\nu(\boldsymbol{k},\sigma)\big) \quad . \tag{1.37}$$

Here we assume box quantization with $\boldsymbol{k} = \left(\frac{2\pi j_1}{L_1}, \ldots, \frac{2\pi j_d}{L_d}\right)$, where j_1 *etc.* are all integers. The volume associated with each point in $\boldsymbol{k}$ space is then $\Delta V = (2\pi/L_1)\cdots(2\pi/L_d) = (2\pi)^d/V$, which establishes the above equality in the thermodynamic limit. We can also restrict our attention to a particular band ν and spin polarization σ, and define

$$g_{\nu\sigma}(\varepsilon) = \int\limits_{\hat{\Omega}} \frac{d^dk}{(2\pi)^d}\, \delta\big(\varepsilon - E_\nu(\boldsymbol{k},\sigma)\big) \quad . \tag{1.38}$$

Finally, we may multiply by the real space unit cell volume v_0 to obtain $\overline{g}(\varepsilon) \equiv v_0\, g(\varepsilon)$, which has dimensions of inverse energy, and gives the number of levels per unit energy per unit cell.

---

[8] Here we denote the band index as ν, to obviate confusion with the occupancy n below.

[9] If there is an external magnetic field H, for example, the energy levels will be spin polarization dependent.

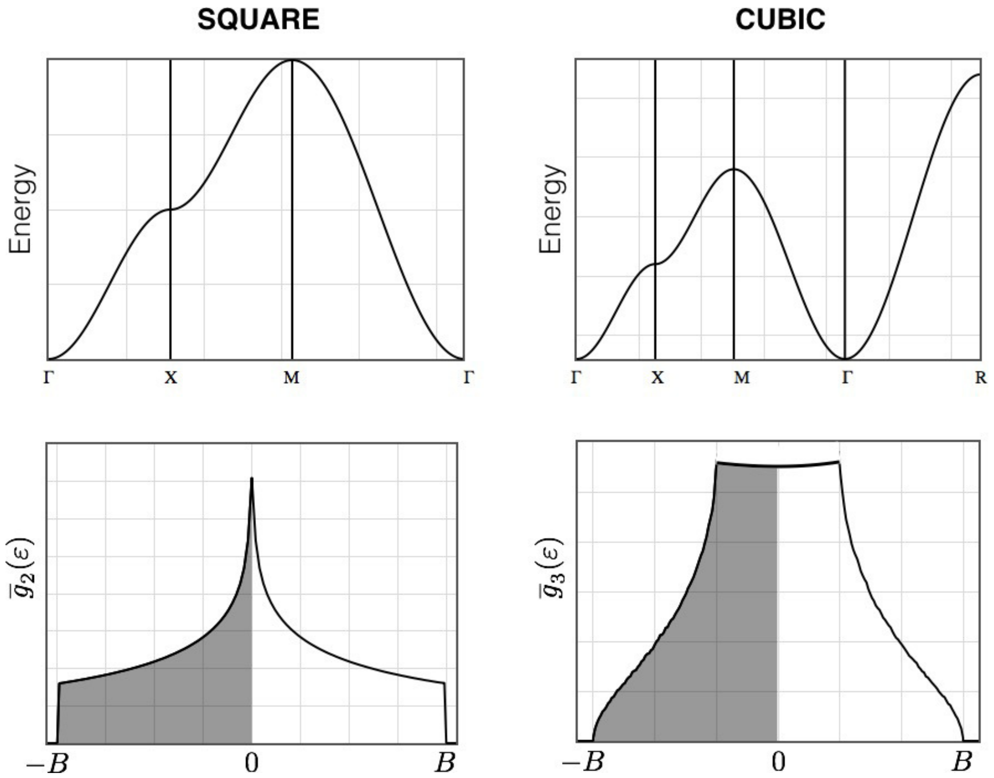

Figure 1.8: Upper left: Two-dimensional dispersion $E(k_x, k_y)$ along high symmetry lines in the 2D square lattice first Brillouin zone. Lower left: Corresponding density of states $\overline{g}_2(\varepsilon)$. Upper right: Three-dimensional dispersion $E(k_x, k_y, k_z)$ along high symmetry lines in the 2D cubic lattice first Brillouin zone. Lower right: Corresponding density of states $\overline{g}_3(\varepsilon)$. Shaded regions show occupied states for a lattice of s-orbitals with one electron per site. Figures from http://lampx.tugraz.at/∼hadley/ss1/bands/tbtable/tbtable.html .

Examples

Consider the case of a one-dimensional band with dispersion $E(k) = -2t\cos(ka)$. The density of states per unit cell is

$$\overline{g}(\varepsilon) = a\int\limits_{-\frac{\pi}{a}}^{\frac{\pi}{a}} \frac{dk}{2\pi}\,\delta(\varepsilon + 2t\cos ka) = \frac{1}{\pi}\,\big(B^2 - \varepsilon^2\big)^{-1/2}\,\Theta(B^2 - \varepsilon^2) \quad , \tag{1.39}$$

where $B = 2t$ is half the bandwidth. *I.e.* the allowed energies are $\varepsilon \in [-B, +B]$. Note the square root singularity in $\overline{g}_{d=1}(\varepsilon)$ at the band edges.

Now let's jump to d space dimensions, and the dispersion $E(\boldsymbol{k}) = -2t\sum_{i=1}^{d}\cos(k_i a)$. The DOS per unit cell is then

$$\overline{g}_d(\varepsilon) = \int\limits_{-\pi}^{\pi} \frac{d\theta_1}{2\pi} \cdots \int\limits_{-\pi}^{\pi} \frac{d\theta_d}{2\pi}\,\delta\big(\varepsilon + 2t\cos\theta_1 + \cdots + 2t\cos\theta_d\big) = \frac{1}{\pi}\int\limits_0^{\infty} du\,\cos(\varepsilon u)\,\big[J_0(2tu)\big]^d \quad , \tag{1.40}$$

where each $\theta_j = k_j a$, and we have invoked an integral representation of the Dirac δ-function. Here $J_0(x)$ is the ordinary Bessel function of the first kind. Since $\int_{-\infty}^{\infty} d\varepsilon\, \cos(\varepsilon u) = 2\pi\, \delta(u)$, it is easy to see that $\int_{-\infty}^{\infty} d\varepsilon\, \overline{g}(\varepsilon) = 1$, *i.e.* that the DOS is correctly normalized. For $d = 2$, the integral may be performed to yield

$$\overline{g}_2(\varepsilon) = \frac{2}{\pi^2 B}\, \mathsf{K}\Big(\sqrt{1-(\varepsilon/B)^2}\Big)\, \Theta(B^2 - \varepsilon^2) \quad , \tag{1.41}$$

where

$$\mathsf{K}(k) = \int_0^{\pi/2} \frac{d\theta}{\sqrt{1-k^2 \sin^2\!\theta}} \tag{1.42}$$

is the complete elliptic integral of the first kind[10], and $B = 4t$ is the half bandwidth. The function $\overline{g}_2(\varepsilon)$ has a logarithmic singularity at the band center $\varepsilon = 0$, called a *van Hove singularity*.

The results for $d = 2$ and $d = 3$ are plotted in Fig. 1.8. The logarithmic van Hove singularity at $\varepsilon = 0$ is apparent in $\overline{g}_2(\varepsilon)$. The function $\overline{g}_3(\varepsilon)$ has van Hove singularities at $\varepsilon = \pm\frac{1}{3}B$, where the derivative $g_3'(\varepsilon)$ is discontinuous. In the limit $d \to \infty$, we can use the fact that $J_0(x) = 1 - \frac{1}{4}x^2 + \ldots$ to extract

$$\overline{g}_{d\gg 1}(\varepsilon) = \sqrt{\frac{d}{\pi B^2}}\, e^{-d\varepsilon^2/B^2} = (4\pi d t^2)^{-1/2}\, \exp\!\big(-\,\varepsilon^2/4dt^2\big) \quad . \tag{1.43}$$

We recognize this result as the Central Limit Theorem in action. With $E(\boldsymbol{k}) = -2t\sum_{i=1}^{d} \cos\theta_i$ and θ_i uniformly distributed along $[-\pi, \pi]$, the standard deviation σ is given by

$$\sigma^2 = (2t)^2 \times d \times \langle \cos^2\!\theta \rangle = 2dt^2 \quad , \tag{1.44}$$

exactly as in Eqn. 1.43

Band edge behavior

In the vicinity of a quadratic band minimum, along principal axes of the effective mass tensor, we have

$$E(\boldsymbol{k}) = \Delta + \sum_{i=1}^{d} \frac{\hbar^2 k_i^2}{2m_i^*} \quad , \tag{1.45}$$

and the density of states is

$$\begin{aligned}\overline{g}(\varepsilon) &= v_0 \!\int\! \frac{dk_1}{2\pi} \cdots \!\int\! \frac{dk_d}{2\pi}\, \delta\bigg(\varepsilon - \Delta - \sum_i \frac{\hbar^2 k_i^2}{2m_i^*}\bigg) \\ &= \frac{v_0}{2} \cdot \frac{\sqrt{2m_1^*}}{h} \cdots \frac{\sqrt{2m_d^*}}{h}\, \Omega_d\, (\varepsilon - \Delta)^{\frac{d}{2}-1} \quad ,\end{aligned} \tag{1.46}$$

where $\Omega_d = 2\pi^{d/2}/\Gamma(d/2)$ is the area of the unit sphere in d space dimensions. Consistent with Fig. 1.8, $g_{d=2}(\varepsilon)$ tends to a constant at the band edges, and then discontinuously drops to zero as one exits the band. In $d = 3$, $\overline{g}_{d=3}(\varepsilon)$ vanishes as $(\varepsilon - \Delta)^{1/2}$ at a band edge.

---

[10] There is an unfortunate notational variation in some sources, which write $K(m)$ in place of $\mathsf{K}(k)$, where $m = k^2$.

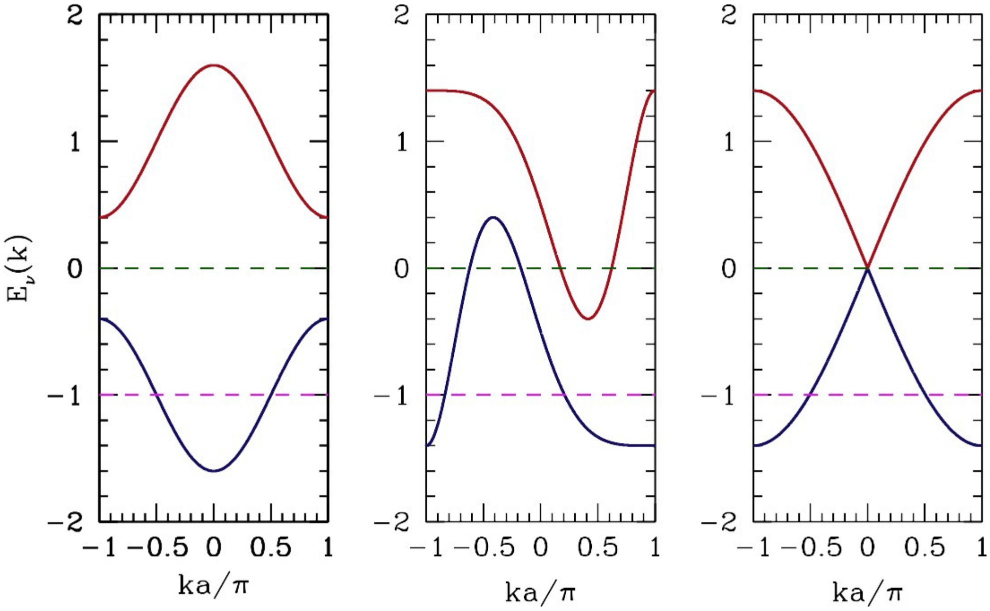

Figure 1.9: Three one-dimensional band structures. Valence bands are shown in dark blue, and conduction bands in dark red. Left: Non-overlapping bands with forbidden region $E \in [-0.4, 0.4]$. Center: At each point there is a direct gap, but the indirect gap is negative and there is no forbidden region. Right: Linear crossing leading to cusp-like band touching. In all cases, when $\varepsilon_{\rm F} = -1$ (dashed magenta line), the Fermi energy cuts through the bottom band and the system is a metal. When $\varepsilon_{\rm F} = 0$ (dashed green line), the system at the left is an insulator, with $g(\varepsilon_{\rm F}) = 0$. The system in the middle is a metal, with $g(\varepsilon_{\rm F}) > 0$ The system on the right, with $g(E)$ vanishing continuously as $\varepsilon \to \varepsilon_{\rm F}$, is called a *semimetal*.

1.3.2 Fermi statistics

If we assume the electrons are noninteracting[11], the energy of the state for which the occupancy of state $|\nu\boldsymbol{k}\sigma\rangle$ is $n_{\nu\boldsymbol{k}\sigma}$ is

$$E\big[\{n_{\nu\boldsymbol{k}\sigma}\}\big] = \sum_\nu \sum_\sigma {\sum_{\boldsymbol{k}}}' E_\nu(\boldsymbol{k},\sigma)\, n_{\nu\boldsymbol{k}\sigma} \quad . \tag{1.47}$$

The Pauli exclusion principle tells us that a given electronic energy level can accommodate at zero or one fermion, which means each $n_{\nu\boldsymbol{k}\sigma}$ is either 0 or 1. At zero temperature, the N electron ground state is obtained by filling up all the energy levels starting from the bottom of the spectrum, with one electron per level, until the lowest N such levels have been filled. In $E_\nu(\boldsymbol{k},\sigma)$ is independent of σ, then there will be a twofold *Kramers degeneracy* whenever N is odd, as the last level filled can either have $\sigma = +1$ or $\sigma = -1$[12].

At finite temperature $T > 0$, the thermodynamic average of $n_{\nu\boldsymbol{k}\sigma}$ is given, within the grand canonical

---

[11] Other, that is, than the mean "Hartree" contribution to the potential $V(\boldsymbol{r})$.

[12] There can be additional degeneracies. For example, in $d = 1$ if, suppressing the band index, $E(k) = E(-k)$, then each level with $k \neq 0$ and $k \neq \pi/a$ is fourfold degenerate: $(k\uparrow,\, k\downarrow,\, -k\uparrow,\, -k\uparrow)$.

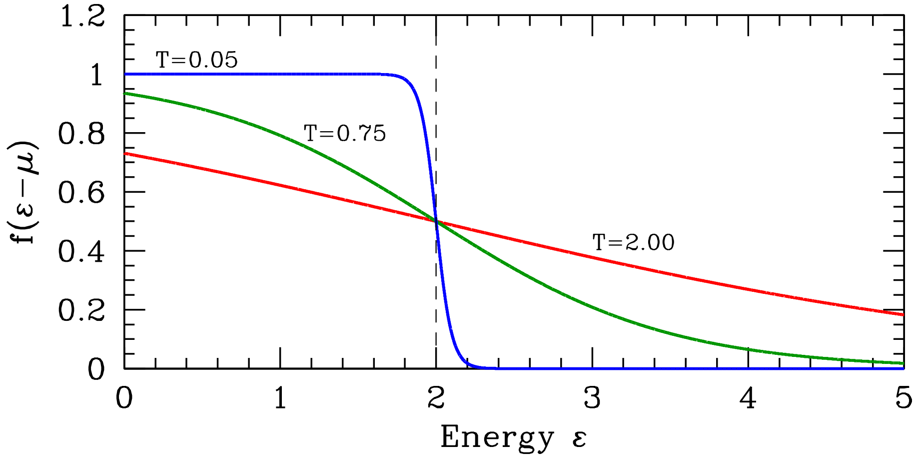

Figure 1.10: The Fermi distribution, $f(x) = \big[\exp(x/k_{\mathrm{B}}T) + 1\big]^{-1}$. Here we have set $k_{\mathrm{B}} = 1$ and taken $\mu = 2$, with $T = \frac{1}{20}$ (blue), $T = \frac{3}{4}$ (green), and $T = 2$ (red). In the $T \to 0$ limit, $f(x)$ approaches a step function $\Theta(-x)$.

ensemble, by

$$\langle n_{\nu\boldsymbol{k}\sigma}\rangle = \frac{1}{\exp\!\Big(\frac{E_\nu(\boldsymbol{k},\sigma)-\mu}{k_{\mathrm{B}}T}\Big)+1} \equiv f\big(E_\nu(\boldsymbol{k},\sigma)-\mu\big) \quad , \tag{1.48}$$

where $f(x)$ is the *Fermi function*,

$$f(x) = \frac{1}{e^{x/k_{\mathrm{B}}T}+1} \quad . \tag{1.49}$$

The total electron number density is then

$$\begin{aligned} n(T,\mu) = \frac{N}{V} &= \int\limits_{-\infty}^{\infty} \! d\varepsilon \, g(\varepsilon)\, f(\varepsilon-\mu) \\ &= \sum_\nu \sum_\sigma \int \frac{d^d k}{(2\pi)^d} \frac{1}{\exp\!\Big(\frac{E_\nu(\boldsymbol{k},\sigma)-\mu}{k_{\mathrm{B}}T}\Big)+1} \quad . \end{aligned} \tag{1.50}$$

This is a Gibbs-Duhem relation, involving the three intensive quantities (n,T,μ). In principle it can be inverted to yield the chemical potential $\mu(n,T)$ as a function of number density and temperature. When $T=0$, we write $\mu(n,T=0) \equiv \varepsilon_{\mathrm{F}}$, which is the *Fermi energy*. Since the Fermi function becomes $f(x) = \Theta(-x)$ at zero temperature, we have

$$n(\varepsilon_{\mathrm{F}}) = \int\limits_{-\infty}^{\varepsilon_{\mathrm{F}}} \! d\varepsilon \, g(\varepsilon) \quad . \tag{1.51}$$

This is to be inverted to obtain $\mu(n,T=0) = \varepsilon_{\mathrm{F}}(n)$.

1.3.3 Metals and insulators at $T = 0$

At $T = 0$, the ground state is formed by filling up each single particle state $|\, n\boldsymbol{k}\sigma \,\rangle$ until the source of electrons (*i.e.* the atoms) is exhausted. Suppose there are N_e electrons in total. If there is a finite gap Δ between the N_e^th and $(N_\mathrm{e} + 1^\mathrm{th}$ energy states, the material is an *insulator*. If the gap is zero, the material is a *metal* or possibly a *semimetal*. For a metal, $g(\varepsilon_\mathrm{F}) > 0$, whereas for a semimetal, $g(\varepsilon_\mathrm{F}) = 0$ but $g(\varepsilon) \sim |\varepsilon - \varepsilon_\mathrm{F}|^\alpha$ as $\varepsilon \to \varepsilon_\mathrm{F}$, where $\alpha > 0$.

Under periodic boundary conditions, there are N quantized wavevectors $\boldsymbol{k}$ in each Brillouin zone, where N is the number of unit cells in the crystal. Since, for a given band index n and wavevector $\boldsymbol{k}$ we can accommodate a maximum of two electrons, one with spin $\uparrow$ and the second with spin $\downarrow$, each band can accommodate a total of $2N$ electrons. Thus, if the number of electrons per cell N_e/N is not a precise multiple of two, then *necessarily* at least one of the bands will be partially filled, which means the material is a metal. Typically we only speak of valence and conduction electrons, since the core bands are all fully occupied and the high energy bands are all completely empty. Then we can define the *electron filling factor* $\nu = \widetilde{N}_\mathrm{e}/N$, where $\widetilde{N}_\mathrm{e}$ is the total number of valence plus conduction electrons. As we have just noted, if $\nu \neq 2k$ for some $k \in \mathbb{Z}$, the material is a metal.

Is the converse also the case, *i.e.* if $\nu = 2k$ is the material always an insulator? It ain't necessarily so! As the middle panel of Fig. 1.9 shows, it is at least in principle possible to have an arrangement of several partially filled bands such that the total number of electrons per site is an even integer. This is certainly a nongeneric state of affairs, but it is not completely ruled out.

1.4 Calculation of Energy Bands

1.4.1 The tight binding model

A crystal is a regular assembly of atoms, which are bound in the crystalline state due to the physics of electrostatics and quantum mechanics. Consider for the sake of simplicity a homonuclear Bravais lattice, *i.e.* a crystalline lattice in which there is the same type of atom at every lattice site, and in which all lattice sites are equivalent under translation. As the lattice constant a tends to infinity, the electronic energy spectrum of the crystal is the same as that of each atom, with an extensive degeneracy of N, the number of unit cells in the lattice. For finite a, the atomic orbitals on different lattice sites will overlap. Initially we will assume a Bravais lattice, but further below we shall generalize this to include the possibility of a basis.

Let $|\, n\boldsymbol{R}\,)$ denote an atomic orbital at Bravais lattice site $\boldsymbol{R}$, where $n \in \{1\mathrm{s}, 2\mathrm{s}, 2\mathrm{p}, \ldots\}$. The atomic wavefunctions[13],

$$\varphi_{n\boldsymbol{R}}(\boldsymbol{r}) = (\, \boldsymbol{r} \,|\, n\boldsymbol{R} \,) = \varphi_n(\boldsymbol{r} - \boldsymbol{R}) \quad , \tag{1.52}$$

Atomic orbitals on the same site form an orthonormal basis: $(\, n\boldsymbol{R} \,|\, n'\boldsymbol{R} \,) = \delta_{nn'}$. However, orbitals on

---

[13] In our notation, $|\, \boldsymbol{r} \,) = |\, \boldsymbol{r} \,\rangle$, so $(\, \boldsymbol{r} \,|\, \boldsymbol{r}' \,) = \delta(\boldsymbol{r} - \boldsymbol{r}')$.

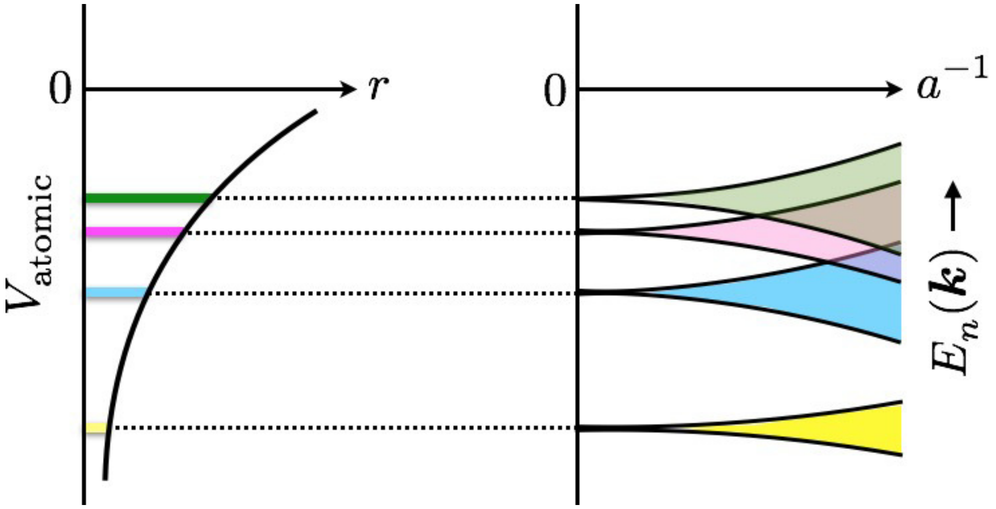

Figure 1.11: Left: Atomic energy levels. Right: Dispersion of crystalline energy bands as a function of interatomic separation.

different lattice sites are not orthogonal, and satisfy

$$(\,n\boldsymbol{R}\,|\,n'\boldsymbol{R}'\,) = \int\! d^d r\; \varphi^*_n(\boldsymbol{r}-\boldsymbol{R})\,\varphi_{n'}(\boldsymbol{r}-\boldsymbol{R}') \equiv S_{nn'}(\boldsymbol{R}-\boldsymbol{R}') \quad , \tag{1.53}$$

where $S_{nn'}(\boldsymbol{R}-\boldsymbol{R}')$ is the *overlap matrix*. Note that $S_{nn'}(0)=\delta_{nn'}$. If we expand the wavefunction $|\,\psi\,\rangle = \sum_{n,\boldsymbol{R}} C_{n\boldsymbol{R}}\,|\,n\boldsymbol{R}\,)$ in atomic orbitals, the Schrödinger equation takes the form

$$\sum_{n',\boldsymbol{R}'} \Big\{ \overbrace{(\,n\boldsymbol{R}\,|\,H\,|\,n'\boldsymbol{R}'\,)}^{H_{nn'}(\boldsymbol{R}-\boldsymbol{R}')} - E\, \overbrace{(\,n\boldsymbol{R}\,|\,n'\boldsymbol{R}'\,)}^{S_{nn'}(\boldsymbol{R}-\boldsymbol{R}')} \Big\}\, C_{n'\boldsymbol{R}'} = 0 \quad , \tag{1.54}$$

where

$$\begin{aligned} H_{nn'}(\boldsymbol{R}-\boldsymbol{R}') &= (\,n\boldsymbol{R}\,|\,H\,|\,n'\boldsymbol{R}'\,) \\ &= \int\! d^d r\; \varphi^*_n(\boldsymbol{r}-\boldsymbol{R}) \left\{ -\frac{\hbar^2}{2m}\nabla^2 + V(\boldsymbol{r}) \right\} \varphi_{n'}(\boldsymbol{r}-\boldsymbol{R}') \quad , \end{aligned} \tag{1.55}$$

where $V(\boldsymbol{r}) = \sum_{\boldsymbol{R}} v(\boldsymbol{r}-\boldsymbol{R})$ is the lattice potential. Note that

$$\begin{aligned} H_{nn'}(\boldsymbol{R}) = \tfrac{1}{2}\Big[E^{\rm at}_n + E^{\rm at}_{n'}\Big]\, S_{nn'}(\boldsymbol{R}) &+ \tfrac{1}{2}\!\int\! d^d r\; \varphi^*_n(\boldsymbol{r}-\boldsymbol{R})\, \Big[v(\boldsymbol{r}) + v(\boldsymbol{r}-\boldsymbol{R})\Big]\, \varphi_{n'}(\boldsymbol{r}) \\ &+ \sum_{\substack{\boldsymbol{R}' \\ (\neq 0,\boldsymbol{R})}} \int\! d^d r\; \varphi^*_n(\boldsymbol{r}-\boldsymbol{R})\, v(\boldsymbol{r}-\boldsymbol{r}')\, \varphi_{n'}(\boldsymbol{r}) \quad . \end{aligned} \tag{1.56}$$

We can simplify Eqn. 1.54 a bit by utilizing the translational invariance of the Hamiltonian and overlap matrices. We write $C_{n\boldsymbol{R}} = C_n(\boldsymbol{k})\,\exp(i\boldsymbol{k}\cdot\boldsymbol{R})$, as well as

$$\widehat{S}_{nn'}(\boldsymbol{k}) = \sum_{\boldsymbol{R}} e^{-i\boldsymbol{k}\cdot\boldsymbol{R}}\, S_{nn'}(\boldsymbol{R}) \qquad , \qquad \widehat{H}_{nn'}(\boldsymbol{k}) = \sum_{\boldsymbol{R}} e^{-i\boldsymbol{k}\cdot\boldsymbol{R}}\, H_{nn'}(\boldsymbol{R}) \quad . \tag{1.57}$$

The Schrödinger equation then separates for each $\boldsymbol{k}$ value, *viz.*

$$\sum_{n'} \Big\{ \widehat{H}_{nn'}(\boldsymbol{k}) - E(\boldsymbol{k})\, \widehat{S}_{nn'}(\boldsymbol{k}) \Big\}\, C_{n'}(\boldsymbol{k}) \quad . \tag{1.58}$$

Note that

$$\widehat{H}^*_{n'n}(\boldsymbol{k}) = \sum_{\boldsymbol{R}} e^{i\boldsymbol{k}\cdot\boldsymbol{R}}\, H^*_{n'n}(\boldsymbol{R}) = \sum_{\boldsymbol{R}} e^{i\boldsymbol{k}\cdot\boldsymbol{R}}\, H_{nn'}(-\boldsymbol{R}) = \widehat{H}_{nn'}(\boldsymbol{k}) \quad , \tag{1.59}$$

hence for each $\boldsymbol{k}$, the matrices $\widehat{H}_{nn'}(\boldsymbol{k})$ and $\widehat{S}_{nn'}(\boldsymbol{k})$ are Hermitian.

Suppose we ignore the overlap between different bands. We can then suppress the band index, and write[14]

$$\begin{aligned} S(\boldsymbol{R}) &= \int \! d^d r\; \varphi^*(\boldsymbol{r} - \boldsymbol{R})\, \varphi(\boldsymbol{r}) \\ H(\boldsymbol{R}) &= E^{\text{at}}\, S(\boldsymbol{R}) + \sum_{\boldsymbol{R}'\neq 0} \int \! d^d r\; \varphi^*(\boldsymbol{r} - \boldsymbol{R})\, v(\boldsymbol{r} - \boldsymbol{R}')\, \varphi(\boldsymbol{r}) \quad ; \end{aligned} \tag{1.60}$$

Note that $S(0) = 1$. The tight binding dispersion is then

$$E(\boldsymbol{k}) = \frac{\widehat{H}(\boldsymbol{k})}{\widehat{S}(\boldsymbol{k})} = E^{\text{at}} - \frac{\sum_{\boldsymbol{R}} t(\boldsymbol{R})\, e^{-i\boldsymbol{k}\cdot\boldsymbol{R}}}{\sum_{\boldsymbol{R}} S(\boldsymbol{R})\, e^{-i\boldsymbol{k}\cdot\boldsymbol{R}}} \quad , \tag{1.61}$$

where

$$t(\boldsymbol{R}) = E^{\text{at}} - H(\boldsymbol{R}) = -\int \! d^d r\; \varphi^*(\boldsymbol{r} - \boldsymbol{R}) \Bigg[\sum_{\boldsymbol{R}'\neq 0} v(\boldsymbol{r} - \boldsymbol{R}') \Bigg] \varphi(\boldsymbol{r}) \quad . \tag{1.62}$$

Let's examine this result for a d-dimensional cubic lattice. To simplify matters, we assume that $t(\boldsymbol{R})$ and $S(\boldsymbol{R})$ are negligible beyond the nearest neighbor separation $|\boldsymbol{R}| = a$. Then

$$\begin{aligned} E(\boldsymbol{k}) &= E^{\text{at}} - \frac{t(0) + 2\, t(a) \sum_{j=1}^{d} \cos(k_j a)}{1 + 2\, S(a) \sum_{j=1}^{d} \cos(k_j a)} \\ &\approx E^{\text{at}} - t(0) - 2\big[t(a) - t(0) S(a) \big] \sum_{j=1}^{d} \cos(k_j a) + \ldots \quad , \end{aligned} \tag{1.63}$$

where we expand in the small quantity $S(a)$.

Remarks

Eqn. 1.58 says that the eigenspectrum of the crystalline Hamiltonian at each crystal momentum $\boldsymbol{k}$ is obtained by simultaneously diagonalizing the matrices $\widehat{H}(\boldsymbol{k})$ and $\widehat{S}(\boldsymbol{k})$. Thus, we should seek, for each

---

[14] The student should derive the formulae in Eqn. 1.60. In so doing, is it necessary to presume that the atomic wavefunctions are each of a definite parity?

$\boldsymbol{k}$, a matrix $\Lambda_{nl}(\boldsymbol{k})$ such that[15]

$$\Lambda^{-1}_{an}(\boldsymbol{k})\,\widehat{H}_{nn'}(\boldsymbol{k})\,\Lambda_{n'a'}(\boldsymbol{k}) = h_a(\boldsymbol{k})\,\delta_{aa'} \qquad , \qquad \Lambda^{-1}_{an}(\boldsymbol{k})\,\widehat{S}_{nn'}(\boldsymbol{k})\,\Lambda_{n'a'}(\boldsymbol{k}) = s_a(\boldsymbol{k})\,\delta_{aa'} \quad . \tag{1.64}$$

The band energies are then given by

$$E_a(\boldsymbol{k}) = \frac{h_a(\boldsymbol{k})}{s_a(\boldsymbol{k})} \quad . \tag{1.65}$$

This seems straightforward enough. However, implicit in this procedure is the assumption that the overlap matrix is nonsingular, which is clearly wrong! We know that the atomic eigenstates at any *single* lattice site must form a complete set, therefore we must be able to write

$$\varphi_n(\boldsymbol{r}-\boldsymbol{R}) = \sum_{n'} A_{nn'}(\boldsymbol{R})\,\varphi_{n'}(\boldsymbol{r}) \quad . \tag{1.66}$$

Therefore the set $|\,n\boldsymbol{R}\,)$ is massively degenerate. Fortunately, this problem is not nearly so severe as it might first appear. Recall that the atomic eigenstates consist of *bound states* of negative energy, and *scattering states* of positive energy. If we restrict our attention to a finite set of atomic bound states, the overlap matrix remains nonsingular.

1.4.2 Wannier functions

Suppose a very nice person gives us a complete set of Bloch functions $\psi_{n\boldsymbol{k}}(\boldsymbol{r})$. We can then form the linear combinations

$$W_n(\boldsymbol{r}-\boldsymbol{R}) \equiv \frac{1}{\sqrt{N}}\sum_{\boldsymbol{k}} e^{i\chi_n(\boldsymbol{k})}\,e^{-i\boldsymbol{k}\cdot\boldsymbol{R}}\,\psi_{n\boldsymbol{k}}(\boldsymbol{r}) = \frac{1}{\sqrt{N}}\sum_{\boldsymbol{k}} e^{i\chi_n(\boldsymbol{k})}\,e^{i\boldsymbol{k}\cdot(\boldsymbol{r}-\boldsymbol{R})}\,u_{n\boldsymbol{k}}(\boldsymbol{r}) \quad , \tag{1.67}$$

were N is the number of unit cells and $\chi_n(\boldsymbol{k})$ is a smooth function of the wavevector $\boldsymbol{k}$ which satisfies $\chi_n(\boldsymbol{k}+\boldsymbol{G}) = \chi_n(\boldsymbol{k})$. The $\boldsymbol{k}$ sum is over all wavevectors lying within the first Brillouin zone. Writing $W_n(\boldsymbol{r}) = \langle\,\boldsymbol{r}\,|\,n\boldsymbol{R}\,\rangle$, we have

$$|\,n\boldsymbol{R}\,\rangle = \frac{1}{\sqrt{N}}\sum_{\boldsymbol{k}} e^{i\chi_n(\boldsymbol{k})}\,e^{-i\boldsymbol{k}\cdot\boldsymbol{R}}\,|\,n\boldsymbol{k}\,\rangle \quad , \tag{1.68}$$

and the overlap matrix is

$$\langle\,n\boldsymbol{R}\,|\,n'\boldsymbol{R}'\,\rangle = \int\! d^d r\; W^*_n(\boldsymbol{r}-\boldsymbol{R})\,W_{n'}(\boldsymbol{r}-\boldsymbol{R}') = \delta_{nn'}\,\delta_{\boldsymbol{R}\boldsymbol{R}'} \quad . \tag{1.69}$$

The functions $W_n(\boldsymbol{r}-\boldsymbol{R})$ are called *Wannier functions*. They are linear combinations of Bloch states within a single energy band which are localized about a single Bravais lattice site or unit cell. Since the Wannier states are normalized, we have $\int d^d r\,\big|W_n(\boldsymbol{r}-\boldsymbol{R})\big|^2 = 1$, which means, if the falloff is the same in all symmetry-related directions of the crystal, that the envelope of $W_n(\boldsymbol{r}-\boldsymbol{R})$ must decay faster than $|\boldsymbol{r}-\boldsymbol{R}|^{-d/2}$ in d dimensions. For core ionic orbitals such as the 1s states, the atomic wavefunctions themselves are good approximations to Wannier states. Note that our freedom to choose the phase

---

[15] Einstein summation convention for repeated indices is used throughout these notes, unless explicitly stated otherwise. Our first 'otherwise': the index a is not summed in expressions such as $h_a(\boldsymbol{k})\,\delta_{aa'}$.

functions $\chi_n(\boldsymbol{k})$ results in many different possible definitions of the Wannier states. One desideratum we may choose to impose is to constrain the phase functions so as to minimize the expectation of $(\boldsymbol{r}-\boldsymbol{R})^2$ in each band.

Closed form expressions for Wannier functions are hard to come by, but we can obtain results for the case where the cell functions are constant, *i.e.* $u_{n\boldsymbol{k}}(\boldsymbol{r}) = (Nv_0)^{-1/d}$. Consider the cubic lattice case in $d = 3$ dimensions, where $v_0 = a^3$. We then have

$$\begin{aligned}
W(\boldsymbol{r}-\boldsymbol{R}) &= v_0^{1/2} \int\limits_{\hat{\Omega}} \frac{d^3k}{(2\pi)^3}\, e^{i\boldsymbol{k}\cdot(\boldsymbol{r}-\boldsymbol{R})} \\
&= \left[\frac{\sqrt{a}}{2\pi} \int\limits_{-\pi/a}^{\pi/a} dk_x\, e^{ik_x(x-X)} \right] \left[\frac{\sqrt{a}}{2\pi} \int\limits_{-\pi/a}^{\pi/a} dk_y\, e^{ik_y(y-Y)} \right] \left[\frac{\sqrt{a}}{2\pi} \int\limits_{-\pi/a}^{\pi/a} dk_z\, e^{ik_z(z-Z)} \right] \\
&= \left[\frac{\sqrt{a}\,\sin\big[\frac{\pi}{a}(x-X)\big]}{\pi(x-X)} \right] \left[\frac{\sqrt{a}\,\sin\big[\frac{\pi}{a}(y-Y)\big]}{\pi(y-Y)} \right] \left[\frac{\sqrt{a}\,\sin\big[\frac{\pi}{a}(z-Z)\big]}{\pi(z-Z)} \right] \quad ,
\end{aligned} \tag{1.70}$$

which falls off as $|\Delta x\, \Delta y\, \Delta z|^{-1}$ along a general direction in space[16].

The Wannier states are not eigenstates of the crystal Hamiltonian. Indeed, we have

$$\begin{aligned}
\langle\, n\boldsymbol{R} \,|\, H \,|\, n'\boldsymbol{R}' \,\rangle &= \frac{1}{N} \sum_{\boldsymbol{k},\boldsymbol{k}'} e^{-i\chi_n(\boldsymbol{k})}\, e^{i\chi_{n'}(\boldsymbol{k}')}\, e^{i\boldsymbol{k}\cdot\boldsymbol{R}}\, e^{-i\boldsymbol{k}'\cdot\boldsymbol{R}'} \langle\, n\boldsymbol{k} \,|\, H \,|\, n'\boldsymbol{k}' \,\rangle \\
&= \delta_{nn'}\, v_0 \int \frac{d^dk}{(2\pi)^d}\, e^{i\boldsymbol{k}\cdot(\boldsymbol{R}-\boldsymbol{R}')}\, E_n(\boldsymbol{k}) \quad ,
\end{aligned} \tag{1.71}$$

which is diagonal in the band indices, but not in the unit cell labels.

1.4.3 Tight binding redux

Suppose we have an orthonormal set of orbitals $|\, a\boldsymbol{R} \,\rangle$, where a labels the orbital and $\boldsymbol{R}$ denotes a Bravais lattice site. The label a may refer to different orbitals associated with the atom at $\boldsymbol{R}$, or it may label orbitals on other atoms in the unit cell defined by $\boldsymbol{R}$. The most general tight binding Hamiltonian we can write is

$$H = \sum_{\boldsymbol{R},\boldsymbol{R}'} \sum_{a,a'} H_{aa'}(\boldsymbol{R}-\boldsymbol{R}')\, |\, a\boldsymbol{R} \,\rangle\langle\, a'\boldsymbol{R}' \,| \quad , \tag{1.72}$$

where $H_{aa'}(\boldsymbol{R}-\boldsymbol{R}') = H^*_{a'a}(\boldsymbol{R}'-\boldsymbol{R}) = \langle\, a, \boldsymbol{R} \,|\, H \,|\, a', \boldsymbol{R}' \,\rangle$ is the Hamiltonian matrix, whose rows and columns are indexed by a composite index combining both the unit cell label $\boldsymbol{R}$ and the orbital label a. When $\boldsymbol{R} = \boldsymbol{R}'$ and $a = a'$, the term $H_{aa}(0) = \varepsilon_a$ is the energy of a single electron in an isolated a orbital. For all other cases, $H_{aa'}(\boldsymbol{R}-\boldsymbol{R}') = -t_{aa'}(\boldsymbol{R}-\boldsymbol{R}')$ is the hopping integral between the a orbital in unit cell $\boldsymbol{R}$ and the a' orbital in unit cell $\boldsymbol{R}'$. Let's write an eigenstate $|\, \psi \,\rangle$ as

$$|\, \psi \,\rangle = \sum_{\boldsymbol{R}} \sum_{a} \psi_{a\boldsymbol{R}}\, |\, a\boldsymbol{R} \,\rangle \quad . \tag{1.73}$$

---

[16] Note that $W(x,0,0)$ falls off only as $1/|x|$. Still, due to the more rapid decay along a general real space direction, $W(\boldsymbol{r})$ is square integrable.

Applying the Hamiltonian to $|\,\psi\,\rangle$, we obtain the coupled equations

$$\sum_{\boldsymbol{R},\boldsymbol{R}'}\sum_{a,a'} H_{aa'}(\boldsymbol{R}-\boldsymbol{R}')\,\psi_{a'\boldsymbol{R}'}\,|\,a\boldsymbol{R}\,\rangle = E\sum_{\boldsymbol{R}}\sum_{a}\psi_{a\boldsymbol{R}}\,|\,a\boldsymbol{R}\,\rangle \quad . \tag{1.74}$$

Since the $|\,a\boldsymbol{R}\,\rangle$ basis is complete, we must have that the coefficients of $|\,a\boldsymbol{R}\,\rangle$ on each side agree. Therefore,

$$\sum_{\boldsymbol{R}'}\sum_{a'} H_{aa'}(\boldsymbol{R}-\boldsymbol{R}')\,\psi_{a'\boldsymbol{R}'} = E\,\psi_{a\boldsymbol{R}} \quad . \tag{1.75}$$

We now use Bloch's theorem, which says that each eigenstate may be labeled by a wavevector $\boldsymbol{k}$, with $\psi_{a\boldsymbol{R}} = \frac{1}{\sqrt{N}}\,u_a(\boldsymbol{k})\,e^{i\boldsymbol{k}\cdot\boldsymbol{R}}$. The $N^{-1/2}$ prefactor is a normalization term. Multiplying each side by by $e^{-i\boldsymbol{k}\cdot\boldsymbol{R}}$, we have

$$\sum_{a'}\bigg(\sum_{\boldsymbol{R}'} H_{aa'}(\boldsymbol{R}-\boldsymbol{R}')\,e^{-i\boldsymbol{k}\cdot(\boldsymbol{R}-\boldsymbol{R}')}\bigg)\,u_{a'\boldsymbol{k}} = E(\boldsymbol{k})\,u_{a\boldsymbol{k}} \quad , \tag{1.76}$$

which may be written as

$$\sum_{a'}\hat{H}_{aa'}(\boldsymbol{k})\,u_{a'}(\boldsymbol{k}) = E(\boldsymbol{k})\,u_a(\boldsymbol{k}) \quad , \tag{1.77}$$

where

$$\hat{H}_{aa'}(\boldsymbol{k}) = \sum_{\boldsymbol{R}} H_{aa'}(\boldsymbol{R})\,e^{-i\boldsymbol{k}\cdot\boldsymbol{R}} \quad . \tag{1.78}$$

Thus, for each crystal wavevector $\boldsymbol{k}$, the $u_{a\boldsymbol{k}}$ are the eigenfunctions of the $r\times r$ Hermitian matrix $\hat{H}_{aa'}(\boldsymbol{k})$. The energy eigenvalues at wavevector $\boldsymbol{k}$ are given by $\mathsf{spec}\big(\hat{H}(\boldsymbol{k})\big)$, *i.e.* by the set of eigenvalues of the matrix $\hat{H}(\boldsymbol{k})$. There are r such solutions (some of which may be degenerate), which we distinguish with a band index n, and we denote $u_{na}(\boldsymbol{k})$ and $E_n(\boldsymbol{k})$ as the corresponding eigenvectors and eigenvalues. We sometimes will use the definition $\hat{t}_{aa'}(\boldsymbol{k}) \equiv -\hat{H}_{aa'}(\boldsymbol{k})$ for the matrix of hopping integrals.

1.4.4 Interlude on Fourier transforms

It is convenient to use second quantized notation and write the Hamiltonian as

$$H = \sum_{\boldsymbol{R},\boldsymbol{R}'}\sum_{a,a'} H_{aa'}(\boldsymbol{R}-\boldsymbol{R}')\,c^{\dagger}_{a\boldsymbol{R}}\,c_{a'\boldsymbol{R}'} \quad , \tag{1.79}$$

where $c^{\dagger}_{a\boldsymbol{R}}$ creates an electron in orbital a at unit cell $\boldsymbol{R}$. The *second quantized* fermion creation and annihilation operators satisfy the anticommutation relations

$$\big\{c_{a\boldsymbol{R}}\,,\,c^{\dagger}_{a'\boldsymbol{R}'}\big\} = \delta_{\boldsymbol{R}\boldsymbol{R}'}\,\delta_{aa'} \quad . \tag{1.80}$$

To quantize the wavevectors, we place our system on a d-dimensional torus with N_j unit cells along principal Bravais lattice vector $\boldsymbol{a}_j$ for all $j \in \{1,\ldots,d\}$. The total number of unit cells is then $N = N_1N_2\cdots N_d$. Consider now the Fourier transforms,

$$c_{a\boldsymbol{R}} = \frac{1}{\sqrt{N}}\sum_{\boldsymbol{k}} c_{a\boldsymbol{k}}\,e^{i\boldsymbol{k}\cdot\boldsymbol{R}} \qquad , \qquad c^{\dagger}_{a\boldsymbol{R}} = \frac{1}{\sqrt{N}}\sum_{\boldsymbol{k}} c^{\dagger}_{a\boldsymbol{k}}\,e^{-i\boldsymbol{k}\cdot\boldsymbol{R}} \quad . \tag{1.81}$$

and their inverses

$$c_{a\boldsymbol{k}} = \frac{1}{\sqrt{N}} \sum_{\boldsymbol{R}} c_{a\boldsymbol{R}}\, e^{-i\boldsymbol{k}\cdot\boldsymbol{R}} \qquad , \qquad c^\dagger_{a\boldsymbol{k}} = \frac{1}{\sqrt{N}} \sum_{\boldsymbol{R}} c^\dagger_{a\boldsymbol{R}}\, e^{i\boldsymbol{k}\cdot\boldsymbol{R}} \quad . \tag{1.82}$$

One then has $\big\{ c_{a\boldsymbol{k}}\, ,\, c_{a'\boldsymbol{k}'} \big\} = \delta_{aa'}\, \delta_{\boldsymbol{k}\boldsymbol{k}'}$, which says that the Fourier space operators satisfy the same anticommutation relations as in real space, *i.e.* the individual $\boldsymbol{k}$ modes are orthonormal. This is equivalent to the result $\langle\, a\boldsymbol{k} \,|\, a'\boldsymbol{k}' \,\rangle = \delta_{aa'}\, \delta_{\boldsymbol{k}\boldsymbol{k}'}$, where $|\, a\boldsymbol{k}\,\rangle = N^{-1/2} \sum_{\boldsymbol{R}} |\, a\boldsymbol{R}\,\rangle\, e^{-i\boldsymbol{k}\cdot\boldsymbol{R}}$. The Hamiltonian may now be expressed as

$$H = \sum_{\boldsymbol{k}} \sum_{a,a'} \hat{H}_{aa'}(\boldsymbol{k})\, c^\dagger_{a\boldsymbol{k}}\, c_{a'\boldsymbol{k}} \quad , \tag{1.83}$$

where $\hat{H}_{aa'}(\boldsymbol{k})$ was defined in Eqn. 1.78 above.

You must, at the very deepest level of your soul, internalize Eqn. 1.81. Equivalently, using bra and ket vectors,

$$\langle\, a\boldsymbol{R} \,| = \frac{1}{\sqrt{N}} \sum_{\boldsymbol{k}} \langle\, a\boldsymbol{k} \,|\, e^{i\boldsymbol{k}\cdot\boldsymbol{R}} \qquad , \qquad |\, a\boldsymbol{R} \,\rangle = \frac{1}{\sqrt{N}} \sum_{\boldsymbol{k}} |\, a\boldsymbol{k} \,\rangle\, e^{-i\boldsymbol{k}\cdot\boldsymbol{R}} \quad . \tag{1.84}$$

and

$$\langle\, a\boldsymbol{k} \,| = \frac{1}{\sqrt{N}} \sum_{\boldsymbol{R}} \langle\, a\boldsymbol{R} \,|\, e^{-i\boldsymbol{k}\cdot\boldsymbol{R}} \qquad , \qquad |\, a\boldsymbol{k} \,\rangle = \frac{1}{\sqrt{N}} \sum_{\boldsymbol{R}} |\, a\boldsymbol{R} \,\rangle\, e^{i\boldsymbol{k}\cdot\boldsymbol{R}} \quad . \tag{1.85}$$

To establish the inverse relations, we evaluate

$$\begin{aligned} |\, a\boldsymbol{R} \,\rangle &= \frac{1}{\sqrt{N}} \sum_{\boldsymbol{k}} |\, a\boldsymbol{k} \,\rangle\, e^{-i\boldsymbol{k}\cdot\boldsymbol{R}} \\ &= \frac{1}{\sqrt{N}} \sum_{\boldsymbol{k}} \bigg(\frac{1}{\sqrt{N}} \sum_{\boldsymbol{R}'} |\, a\boldsymbol{R}' \,\rangle\, e^{i\boldsymbol{k}\cdot\boldsymbol{R}'} \bigg)\, e^{-i\boldsymbol{k}\cdot\boldsymbol{R}} \\ &= \sum_{\boldsymbol{R}'} \bigg(\frac{1}{N} \sum_{\boldsymbol{k}} e^{-i\boldsymbol{k}\cdot(\boldsymbol{R}-\boldsymbol{R}')} \bigg)\, |\, a\boldsymbol{R}' \,\rangle \quad . \end{aligned} \tag{1.86}$$

Similarly, we find

$$|\, a\boldsymbol{k} \,\rangle = \sum_{\boldsymbol{k}'} \bigg(\frac{1}{N} \sum_{\boldsymbol{R}} e^{i(\boldsymbol{k}-\boldsymbol{k}')\cdot\boldsymbol{R}} \bigg)\, |\, a\boldsymbol{k}' \,\rangle \quad . \tag{1.87}$$

In order for the inverse relations to be true, then, the quantities in round brackets in the previous two equations must satisfy

$$\frac{1}{N} \sum_{\boldsymbol{k}} e^{-i\boldsymbol{k}\cdot(\boldsymbol{R}-\boldsymbol{R}')} = \delta_{\boldsymbol{R}\boldsymbol{R}'} \qquad , \qquad \frac{1}{N} \sum_{\boldsymbol{R}} e^{i(\boldsymbol{k}-\boldsymbol{k}')\cdot\boldsymbol{R}} = \delta_{\boldsymbol{k}\boldsymbol{k}'} \quad . \tag{1.88}$$

Let's see how this works in the $d = 1$ case. Let the lattice constant be a and place our system on a ring of N sites (*i.e.* a one-dimensional torus). The k values are then quantized according to $k_j = 2\pi j/a$, where $j \in \{0, \ldots, N-1\}$. The first equation in Eqn. 1.88 is then

$$\frac{1}{N} \sum_{j=0}^{N-1} e^{-2\pi i j(n-n')/N} = \delta_{nn'} \quad , \tag{1.89}$$

where we have replaced $\boldsymbol{R}$ by na and $\boldsymbol{R}'$ by $n'a$, with $n, n' \in \{1, \ldots, N\}$. Clearly the above equality holds true when $n = n'$. For $n \neq n'$, let $z = e^{-2\pi i(n-n')/N}$. The sum is $1 + z + \ldots + z^{N-1} = (1 - z^N)/(1 - z)$. But $z^N = 1$ and $z \neq 1$, so the identity is again verified.

If we do not restrict n and n' to be among $\{1, \ldots, N\}$ and instead let their values range freely over the integers, then the formula is still correct, provided we write the RHS as $\delta_{n,n' \bmod N}$. Similarly, we must understand $\delta_{\boldsymbol{R}\boldsymbol{R}'}$ in Eqn. 1.88 to be unity whenever $\boldsymbol{R}' = \boldsymbol{R} + l_1 N_1 \boldsymbol{a}_1 + \ldots + l_d N_d \boldsymbol{a}_d$, where each $l_j \in \mathbb{Z}$, and zero otherwise. Similarly, $\delta_{\boldsymbol{k}\boldsymbol{k}'}$ is unity whenever $\boldsymbol{k}' = \boldsymbol{k} + \boldsymbol{G}$, where $\boldsymbol{G} \in \hat{\mathcal{L}}$ is any reciprocal lattice vector, and zero otherwise.

1.4.5 Examples of tight binding dispersions

One-dimensional lattice

Consider the case of a one-dimensional lattice. The lattice sites lie at positions $X_n = na$ for $n \in \mathbb{Z}$. The hopping matrix elements are $t(j) = t\,\delta_{j,1} + t\,\delta_{j,-1}$, where j is the separation between sites in units of the lattice constant a. Then $\hat{t}(k) = 2t\cos(ka)$ and the dispersion is $E(k) = -2t\cos(ka)$. Equivalently, and quite explicitly,

$$\begin{aligned}
H &= -t \sum_n \Big(|\, n+1 \,\rangle\langle\, n \,| + |\, n \,\rangle\langle\, n+1 \,| \Big) \\
&= -\frac{t}{N} \sum_k \sum_{k'} \sum_n e^{-ik'(n+1)a}\, e^{ikna}\, |\, k \,\rangle\langle\, k' \,| + \text{H.c.} \\
&= -t \sum_k \sum_{k'} \bigg(\frac{1}{N} \sum_n e^{i(k-k')na} \bigg)\, e^{-ik'a}\, |\, k \,\rangle\langle\, k' \,| + \text{H.c.} \\
&= -2t \sum_k \cos(ka)\, |\, k \,\rangle\langle\, k \,| \quad ,
\end{aligned} \tag{1.90}$$

since the term in round brackets is $\delta_{kk'}$, as per Eqn. 1.88.

s-orbitals on cubic lattices

On a Bravais lattice with one species of orbital, there is only one band. Consider the case of s orbitals on a d-dimensional cubic lattice. The hopping matrix elements are

$$t(\boldsymbol{R}) = t \sum_{j=1}^{d} \Big(\delta_{\boldsymbol{R},\boldsymbol{a}_j} + \delta_{\boldsymbol{R},-\boldsymbol{a}_j} \Big) \quad , \tag{1.91}$$

where $\boldsymbol{a}_j = a\,\hat{\mathbf{e}}_j$ is the j^{th} elementary direct lattice vector. Taking the discrete Fourier transform (DFT) as specified in Eqn. 1.78,

$$\hat{t}(\boldsymbol{k}) = 2t \sum_{j=1}^{d} \cos(k_j a) \quad . \tag{1.92}$$

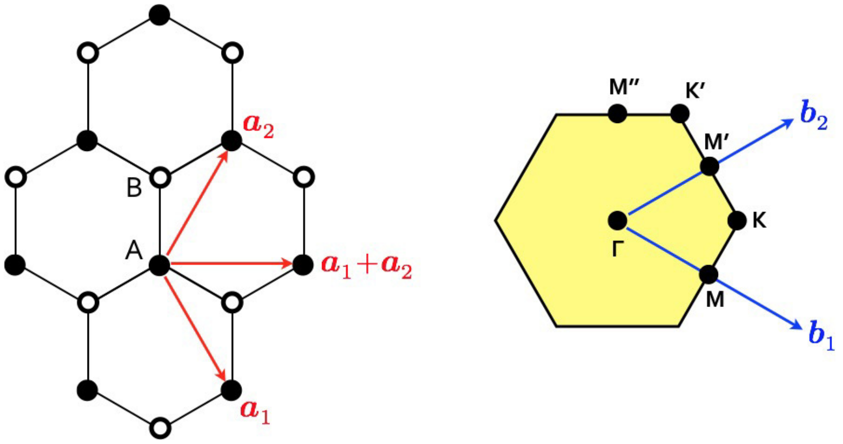

Figure 1.12: Left: The honeycomb lattice is a triangular lattice (black sites) with a two element basis (add white sites). $\boldsymbol{a}_{1,2}$ are elementary direct lattice vectors. Right: First Brillouin zone for the triangular lattice. $\boldsymbol{b}_{1,2}$ are elementary reciprocal lattice vectors. Points of high symmetry Γ, K, K$'$, M, M$'$, and M$''$ are shown.

The dispersion is then $E(\boldsymbol{k}) = -\hat{t}(\boldsymbol{k})$. The model exhibits a *particle-hole symmetry*,

$$\tilde{c}_{\boldsymbol{k}} \equiv c^\dagger_{\boldsymbol{k}+\boldsymbol{Q}} \quad , \tag{1.93}$$

where $\boldsymbol{Q} = \frac{\pi}{a}\big(\hat{\mathbf{e}}_1 + \ldots + \hat{\mathbf{e}}_d\big)$. Note $\hat{t}(\boldsymbol{k}+\boldsymbol{Q}) = -\hat{t}(\boldsymbol{k})$.

s-orbitals on the triangular lattice

The triangular lattice is depicted as the lattice of black dots in the left panel of Fig. 1.12. The elementary direct lattice vectors are

$$\boldsymbol{a}_1 = a\,\big(\tfrac{1}{2}\hat{\mathbf{e}}_1 - \tfrac{\sqrt{3}}{2}\hat{\mathbf{e}}_2\big) \qquad , \qquad \boldsymbol{a}_2 = a\,\big(\tfrac{1}{2}\hat{\mathbf{e}}_1 + \tfrac{\sqrt{3}}{2}\hat{\mathbf{e}}_2\big) \quad , \tag{1.94}$$

and the elementary reciprocal lattice vectors are

$$\boldsymbol{b}_1 = \frac{4\pi}{\sqrt{3}\,a}\,\big(\tfrac{\sqrt{3}}{2}\hat{\mathbf{e}}_1 - \tfrac{1}{2}\hat{\mathbf{e}}_2\big) \qquad , \qquad \boldsymbol{b}_2 = \frac{4\pi}{\sqrt{3}\,a}\,\big(\tfrac{\sqrt{3}}{2}\hat{\mathbf{e}}_1 + \tfrac{1}{2}\hat{\mathbf{e}}_2\big) \quad . \tag{1.95}$$

Note that $\boldsymbol{a}_i \cdot \boldsymbol{b}_j = 2\pi\,\delta_{ij}$. The hopping matrix elements are

$$t(\boldsymbol{R}) = t\,\delta_{\boldsymbol{R},\boldsymbol{a}_1} + t\,\delta_{\boldsymbol{R},-\boldsymbol{a}_1} + t\,\delta_{\boldsymbol{R},\boldsymbol{a}_2} + t\,\delta_{\boldsymbol{R},-\boldsymbol{a}_2} + t\,\delta_{\boldsymbol{R},\boldsymbol{a}_3} + t\,\delta_{\boldsymbol{R},-\boldsymbol{a}_3} \quad , \tag{1.96}$$

where $\boldsymbol{a}_3 \equiv \boldsymbol{a}_1 + \boldsymbol{a}_2$. Thus,

$$\begin{aligned} \hat{t}(\boldsymbol{k}) &= 2t\,\cos(\boldsymbol{k}\cdot\boldsymbol{a}_1) + 2t\,\cos(\boldsymbol{k}\cdot\boldsymbol{a}_2) + 2t\,\cos(\boldsymbol{k}\cdot\boldsymbol{a}_3) \\ &= 2t\cos(\theta_1) + 2t\cos(\theta_2) + 2t\cos(\theta_1+\theta_2) \quad . \end{aligned} \tag{1.97}$$

Here we have written

$$\boldsymbol{k} = \frac{\theta_1}{2\pi}\,\boldsymbol{b}_1 + \frac{\theta_2}{2\pi}\,\boldsymbol{b}_2 + \frac{\theta_3}{2\pi}\,\boldsymbol{b}_3 \quad , \tag{1.98}$$

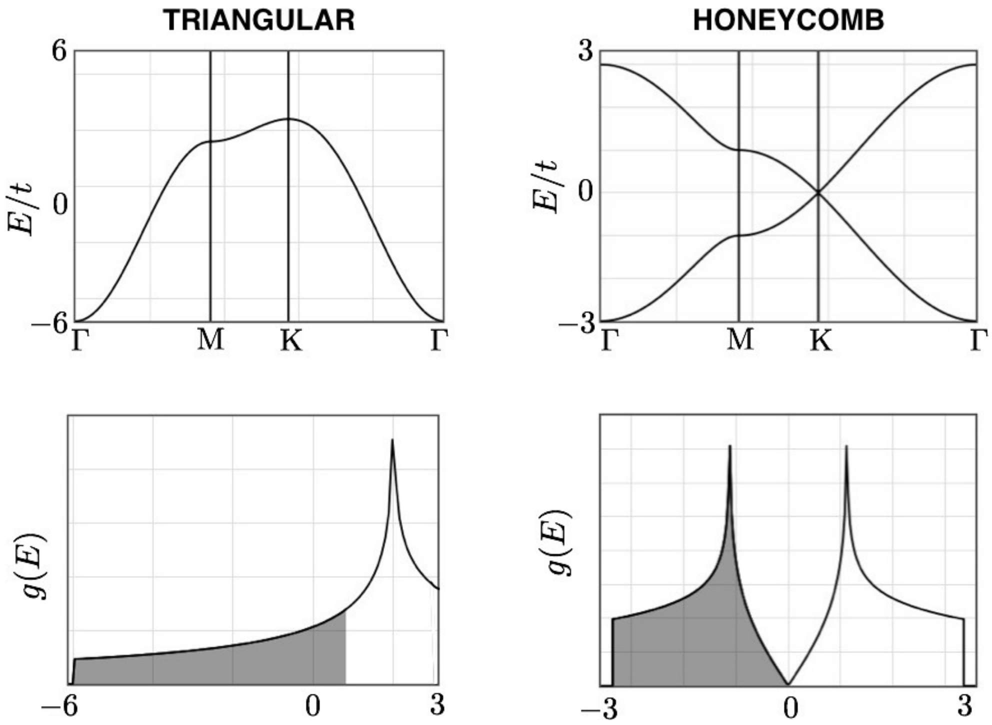

Figure 1.13: Energy bands and density of states for nearest neighbor s-orbital tight binding model on triangular (left) and honeycomb (right) lattices.

and therefore for a general $\boldsymbol{R} = l_1\, \boldsymbol{a}_1 + l_2\, \boldsymbol{a}_2 + l_3\, \boldsymbol{a}_3$, we have

$$\boldsymbol{k} \cdot (l_1 \boldsymbol{a}_1 + l_2 \boldsymbol{a}_2 + l_3 \boldsymbol{a}_3) = l_1\theta_1 + l_2\theta_2 + l_3\theta_3 \quad . \tag{1.99}$$

Again there is only one band, because the triangular lattice is a Bravais lattice. The dispersion relation is $E(\boldsymbol{k}) = -\hat{t}(\boldsymbol{k})$. Unlike the case of the d-dimensional cubic lattice, the triangular lattice energy band does not exhibit particle-hole symmetry. The extrema are at $E_{\text{min}} = E(\Gamma) = -6t$, and $E_{\text{max}} = E(\text{K}) = +3t$, where $\mathit{\Gamma} = 0$ is the zone center and $\text{K} = \frac{1}{3}(\boldsymbol{b}_1 + \boldsymbol{b}_2)$ is the zone corner, corresponding to $\theta_1 = \theta_2 = \frac{2\pi}{3}$.

Graphene: s-orbitals on the honeycomb lattice

Graphene is a two-dimensional form of carbon arrayed in a honeycomb lattice. The electronic structure of carbon is $1\text{s}^2\, 2\text{s}^2\, 2\text{p}^2$. The $1s$ electrons are tightly bound and have small overlaps from site to site, hence little dispersion. The $2s$ and $2p_{x,y}$ orbitals engage in sp^2 hybridization. For each carbon atom, three electrons in each atom's sp^2 orbitals are distributed along bonds connecting to its neighbors[17]. Thus each bond gets two electrons (of opposite spin), one from each of its carbon atoms. This is what chemists call a σ-bond. The remaining p_z orbital (the π orbital, to our chemist friends) is then free to hop from site to site. For our purposes it is equivalent to an s-orbital, so long as we don't ask about its properties under reflection in the x-y plane. The underlying Bravais lattice is triangular, with a two

---

[17] In diamond, the carbon atoms are fourfold coordinated, and th orbitals are sp^3 hybridized.

element basis (labelled A and B in Fig. 1.12). According to the left panel of Fig. 1.12, the A sublattice site in unit cell $\boldsymbol{R}$ is connected to the B sublattice sites in unit cells $\boldsymbol{R}$, $\boldsymbol{R}+\boldsymbol{a}_1$, and $\boldsymbol{R}-\boldsymbol{a}_2$. Thus,

$$t_{\mathsf{AB}}(\boldsymbol{R}) = t\,\delta_{\boldsymbol{R},0} + t\,\delta_{\boldsymbol{R},\boldsymbol{a}_1} + t\,\delta_{\boldsymbol{R}-\boldsymbol{a}_2} \quad , \tag{1.100}$$

and therefore $\hat{t}_{\mathsf{AB}}(\boldsymbol{k}) = t\big(1+e^{i\theta_1}+e^{-i\theta_2}\big)$. We also have $\hat{t}_{\mathsf{BA}}(\boldsymbol{k}) = \hat{t}^*_{\mathsf{AB}}(\boldsymbol{k})$ and $\hat{t}_{\mathsf{AA}}(\boldsymbol{k}) = \hat{t}_{\mathsf{BB}}(\boldsymbol{k}) = 0$. Thus, the Hamiltonian matrix is

$$H(\boldsymbol{k}) = -\begin{pmatrix} 0 & \hat{t}_{\mathsf{AB}}(\boldsymbol{k}) \\ \hat{t}^*_{\mathsf{AB}}(\boldsymbol{k}) & 0 \end{pmatrix} = -t\begin{pmatrix} 0 & 1+e^{i\theta_1}+e^{-i\theta_2} \\ 1+e^{-i\theta_1}+e^{i\theta_2} & 0 \end{pmatrix} \quad , \tag{1.101}$$

and the energy eigenvalues are

$$E_{\pm}(\boldsymbol{k}) = \pm\big|\hat{t}_{\mathrm{AB}}(\boldsymbol{k})\big| = t\sqrt{3+2\cos\theta_1+2\cos\theta_2+2\cos(\theta_1+\theta_2)} \quad . \tag{1.102}$$

These bands are depicted in the right panels of Fig. 1.13. Note the band touching at K (and K′), which are known as *Dirac points*. In the vicinity of either Dirac point, writing $\boldsymbol{k}=\boldsymbol{K}+\boldsymbol{q}$ or $\boldsymbol{k}=\boldsymbol{K}'+\boldsymbol{q}$, one has $E_{\pm}(\boldsymbol{k}) = \hbar v_{\mathrm{F}}|\boldsymbol{q}|$, where $v_{\mathrm{F}} = \frac{\sqrt{3}}{2}\,ta/\hbar$ is the *Fermi velocity*. At the electroneutrality point (*i.e.* one π electron per site), the Fermi levels lies precisely at $\varepsilon_{\mathrm{F}}=0$. The density of states vanishes continuously as one approaches either Dirac point[18].

p-orbitals on the cubic lattice

Finally, consider the case where each site hosts a trio $(p_x\,,\,p_y\,,\,p_z)$ of p-orbitals. Let the separation between two sites be $\boldsymbol{R}$. Then the 3×3 hopping matrix between these sites depends on two tensors, $\delta_{\mu\nu}$ and $\widehat{\boldsymbol{R}}_\mu\widehat{\boldsymbol{R}}_\nu$. When $\hat{\eta}$ lies along one of the principal cubic axes, the situation is as depicted in Fig. 1.14. The hopping matrix is

$$t_{\mu\nu}(\boldsymbol{R}) = t_{\mathrm{w}}(R)\,\delta_{\mu\nu} - \big(t_{\mathrm{w}}(R)+t_{\mathrm{s}}(R)\big)\,\hat{R}_\mu\,\hat{R}_\nu \quad , \tag{1.103}$$

where the weak and strong hoppings $t_{\mathrm{w,s}}$ are depicted in Fig. 1.14. We can now write

$$t_{xx}(\boldsymbol{R}) = -t_{\mathrm{s}}\left(\delta_{\boldsymbol{R},\boldsymbol{a}_1}+\delta_{\boldsymbol{R},-\boldsymbol{a}_1}\right) + t_{\mathrm{w}}\left(\delta_{\boldsymbol{R},\boldsymbol{a}_2}+\delta_{\boldsymbol{R},-\boldsymbol{a}_2}+\delta_{\boldsymbol{R},\boldsymbol{a}_3}+\delta_{\boldsymbol{R},-\boldsymbol{a}_3}\right) \quad , \tag{1.104}$$

and therefore

$$\hat{t}_{\mu\nu}(\boldsymbol{k}) = 2\begin{pmatrix} -t_{\mathrm{s}}\cos\theta_1+t_{\mathrm{w}}(\cos\theta_2+\cos\theta_3) & 0 & 0 \\ 0 & -t_{\mathrm{s}}\cos\theta_2+t_{\mathrm{w}}(\cos\theta_1+\cos\theta_3) & 0 \\ 0 & 0 & -t_{\mathrm{s}}\cos\theta_3+t_{\mathrm{w}}(\cos\theta_1+\cos\theta_2) \end{pmatrix} \tag{1.105}$$

which is diagonal. The three p-band dispersions are given by the diagonal entries.

---

[18] *I.e.*, the DOS in either the K or K′ valley.

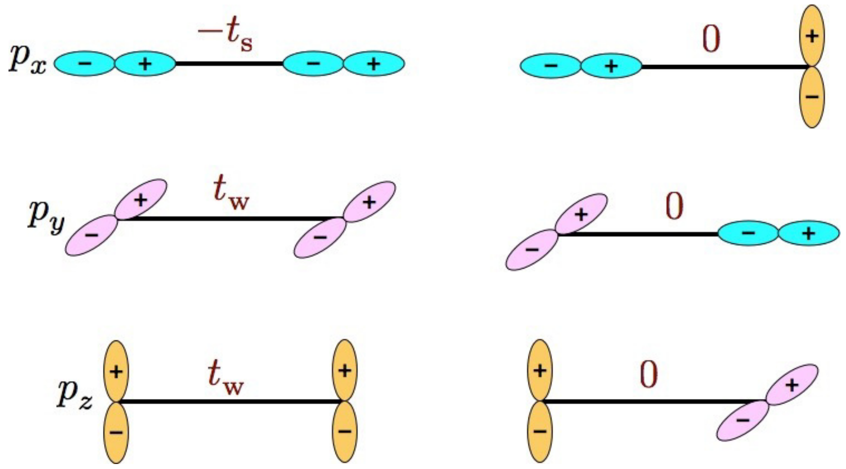

Figure 1.14: Hamiltonian matrix elements for neighboring tight binding orbitals of p symmetry.

1.4.6 Bloch's theorem, again

In Eqn. 1.72,

$$H = \sum_{\boldsymbol{R},\boldsymbol{R}'} \sum_{a,a'} H_{aa'}(\boldsymbol{R}-\boldsymbol{R}')\, |\, a\boldsymbol{R}\rangle\langle\, a'\boldsymbol{R}'\,| \quad ,$$

$\boldsymbol{R}$ and $\boldsymbol{R}'$ labeled Bravais lattice sites, while a and a' labeled orbitals. We stress that these orbitals don't necessarily have to be located on the same ion. We should think of $\boldsymbol{R}$ and $\boldsymbol{R}'$ labeling *unit cells*, each of which is indeed associated with a Bravais lattice site. For example, in the case of graphene, $|\, a\boldsymbol{R}\rangle$ represents an orbital on the a sublattice in unit cell $\boldsymbol{R}$. The eigenvalue equation may be written

$$\hat{H}_{aa'}(\boldsymbol{k})\, u_{na'}(\boldsymbol{k}) = E_n(\boldsymbol{k})\, u_{na}(\boldsymbol{k}) \quad , \tag{1.106}$$

where n is the band index. The function $u_{na}(\boldsymbol{k})$ is the *internal wavefunction* within a given cell, and corresponds to the cell function $u_{n\boldsymbol{k}}(\boldsymbol{r})$ in the continuum, with $a \leftrightarrow (\boldsymbol{r}-\boldsymbol{R})$ labeling a position within each unit cell. The full Bloch state may then be written

$$|\, \psi_{n\boldsymbol{k}}\,\rangle = |\, \boldsymbol{k}\,\rangle \otimes |\, u_{n\boldsymbol{k}}\,\rangle \quad , \tag{1.107}$$

so that

$$\begin{aligned}\psi_{n\boldsymbol{k}}(\boldsymbol{R},a) &= \Big(\langle\, \boldsymbol{R}\,| \otimes \langle\, a\,|\Big)\Big(|\, \boldsymbol{k}\,\rangle \otimes |\, u_{n\boldsymbol{k}}\,\rangle\Big) \\ &= \langle\, \boldsymbol{R}\,|\, \boldsymbol{k}\,\rangle\, \langle\, a\,|\, u_{n\boldsymbol{k}}\,\rangle = \frac{1}{\sqrt{N}}\, e^{i\boldsymbol{k}\cdot\boldsymbol{R}}\, u_{na}(\boldsymbol{k}) \quad .\end{aligned} \tag{1.108}$$

Here we have chosen a normalization $\sum_a \big|u_{na}(\boldsymbol{k})\big|^2 = 1$ within each unit cell, which entails the overall normalization $\sum_{\boldsymbol{R},a} \big|\psi_{n\boldsymbol{k}}(\boldsymbol{R},a)\big|^2 = 1$.

1.5 *Ab initio* Calculations of Electronic Structure

1.5.1 Orthogonalized plane waves

The plane wave expansion of Bloch states in Eqn. 1.10,

$$\psi_{n\boldsymbol{k}}(\boldsymbol{r}) = \sum_{\boldsymbol{G}} C^{(n)}_{\boldsymbol{G}}(\boldsymbol{k})\, e^{i(\boldsymbol{G}+\boldsymbol{k})\cdot\boldsymbol{r}} \tag{1.109}$$

is formally correct, but in practice difficult to implement. The main reason is that one must keep a large number of coefficients $C^{(n)}_{\boldsymbol{G}}(\boldsymbol{k})$ in order to get satisfactory results, because the interesting valence or conduction band Bloch functions must be orthogonal to the core Bloch states derived from the atomic 1s, 2s, *etc.* levels. If the core electrons are localized within a volume v_c, Heisenberg tells us that the spread in wavevector needed to describe such states is given by $\Delta k_x\,\Delta k_y\,\Delta k_z \gtrsim v_\text{c}^{-1}$. In $d=3$, the number of plane waves we need to describe a Bloch state of crystal momentum $\hbar\boldsymbol{k}$ is then

$$N_\text{pw} \approx \frac{\Delta k_x\,\Delta k_y\,\Delta k_z}{\hat{v}_0} = \frac{1}{8\pi^3}\cdot\frac{v_0}{v_\text{c}} \quad , \tag{1.110}$$

where $\hat{v}_0 = \mathsf{vol}(\widehat{\Omega})$ is the volume of the first Brillouin zone (with dimensions $[\hat{v}_0] = L^{-d}$). If the core volume v_c is much smaller than the Wigner-Seitz cell volume v_0, this means we must retain a large number of coefficients in the expansion of Eqn. 1.109.

Suppose, however, an eccentric theorist gives you a good approximation to these core Bloch states. Indeed, according to Eqn. 1.58, if we define $C_n(\boldsymbol{k}) \equiv S^{1/2}_{nn'}(\boldsymbol{k})\, D_{n'}(\boldsymbol{k})$, then the coefficients $D_n(\boldsymbol{k})$ satisfy the eigenvalue equation

$$S^{-1/2}(\boldsymbol{k})\, H(\boldsymbol{k})\, S^{-1/2}(\boldsymbol{k})\boldsymbol{D}_n(\boldsymbol{k}) = E_n(\boldsymbol{k})\,\boldsymbol{D}_n(\boldsymbol{k}) \quad , \tag{1.111}$$

Thus, for each $\boldsymbol{k}$ the eigenvectors $\big\{\boldsymbol{D}_\text{a}(\boldsymbol{k})\big\}$ of the Hermitian matrix $\widetilde{H}(\boldsymbol{k}) \equiv S^{-1/2}(\boldsymbol{k})\, H(\boldsymbol{k})\, S^{-1/2}(\boldsymbol{k})$ yield, upon multiplication by $S^{1/2}(\boldsymbol{k})$, the coefficients $C_n(\boldsymbol{k})$. Here we imagine that the indices n and n' are restricted to the core levels alone. This obviates the subtle problem of overcompleteness of the atomic levels arising from the existence of scattering states. Furthermore, we may write

$$\begin{aligned} S_{nn'}(\boldsymbol{k}) &= \delta_{nn'} + \varSigma_{nn'}(\boldsymbol{k}) \\ \varSigma_{nn'}(\boldsymbol{k}) &= \sum_{\boldsymbol{R}\neq 0} S_{nn'}(\boldsymbol{R})\, e^{-i\boldsymbol{k}\cdot\boldsymbol{R}} \quad , \end{aligned} \tag{1.112}$$

Now since we are talking about core levels, the contribution $\varSigma_{nn'}(\boldsymbol{k})$, which involves overlaps on different sites, is very small. This means the inverse square root, $S^{-1/2} \approx 1 - \frac{1}{2}\varSigma + \mathcal{O}(\varSigma^2)$, can be well-approximated by the first two terms in the expansion in powers of $\varSigma$.

We will write $|\,\mathsf{a}\boldsymbol{k}\,\rangle$ for a core Bloch state in band a, and $|\,\mathsf{a}\boldsymbol{R}\,\rangle$ for the corresponding core Wannier state[19]. Now define the projector,

$$\Pi = \sum_{\mathsf{a},\boldsymbol{k}} |\,\mathsf{a}\boldsymbol{k}\,\rangle\langle\,\mathsf{a}\boldsymbol{k}\,| = \sum_{\mathsf{a},\boldsymbol{R}} |\,\mathsf{a}\boldsymbol{R}\,\rangle\langle\,\mathsf{a}\boldsymbol{R}\,| \quad . \tag{1.113}$$

---

[19] Recall that the Wannier states in a given band are somewhat arbitrary as they depend on a choice of phase.

Note that $\Pi^2 = \Pi$, which is a property of projection operators. We now define

$$|\,\phi_{\boldsymbol{G}+\boldsymbol{k}}\,\rangle \equiv \big(1-\Pi\big)\,|\,\boldsymbol{G}+\boldsymbol{k}\,\rangle \quad , \tag{1.114}$$

where $|\,\boldsymbol{G}+\boldsymbol{k}\,\rangle$ is the plane wave, for which $\langle\,\boldsymbol{r}\,|\,\boldsymbol{G}+\boldsymbol{k}\,\rangle = V^{-1/2}\,e^{i(\boldsymbol{G}+\boldsymbol{k})\cdot\boldsymbol{r}}$. It is important to note that we continue to restrict $\boldsymbol{k}\in\widehat{\mathcal{L}}$ to the first Brillouin zone. Note that $\Pi\,|\phi_{\boldsymbol{G}+\boldsymbol{k}}\rangle = 0$, *i.e.* the state $|\phi_{\boldsymbol{G}+\boldsymbol{k}}\rangle$ has been *orthogonalized* to all the core orbitals. Accordingly, we call

$$\phi_{\boldsymbol{G}+\boldsymbol{k}}(\boldsymbol{r}) = \frac{e^{i(\boldsymbol{G}+\boldsymbol{k})\cdot\boldsymbol{r}}}{\sqrt{V}}\,\Bigg\{1-\sum_{\mathsf{a}} u_{\mathsf{a}\boldsymbol{k}}(\boldsymbol{r})\,e^{-i\boldsymbol{G}\cdot\boldsymbol{r}}\!\!\int\! d^d r'\,u^*_{c\boldsymbol{k}}(\boldsymbol{r}')\,e^{i\boldsymbol{G}\cdot\boldsymbol{r}'}\Bigg\} \tag{1.115}$$

an *orthogonalized plane wave* (OPW).

As an example, consider the case of only a single core 1s orbital, whose atomic wavefunction is given by the hydrogenic form $\varphi(\boldsymbol{r}) = \frac{\alpha^{3/2}}{\sqrt{\pi}}\,e^{-\alpha r}$. The core cell function is then approximately

$$u_{\boldsymbol{k}}(\boldsymbol{r}) \approx \frac{1}{\sqrt{N}}\sum_{\boldsymbol{R}}\varphi(\boldsymbol{r}-\boldsymbol{R})\,e^{-i\boldsymbol{k}\cdot(\boldsymbol{r}-\boldsymbol{R})} \quad . \tag{1.116}$$

We then have

$$\int\! d^3r'\,u^*_{\boldsymbol{k}}(\boldsymbol{r}')\,e^{i\boldsymbol{G}\cdot\boldsymbol{r}'} \approx \sqrt{N}\,\big[\hat{\varphi}(\boldsymbol{G}+\boldsymbol{k})\big]^* = \frac{8\pi^{1/2}\alpha^{5/2}N^{1/2}}{\big[\alpha^2+(\boldsymbol{G}+\boldsymbol{k})^2\big]^2} \tag{1.117}$$

and then

$$\phi_{\boldsymbol{G}+\boldsymbol{k}}(\boldsymbol{r}) = \frac{e^{i(\boldsymbol{G}+\boldsymbol{k})\cdot\boldsymbol{r}}}{\sqrt{V}}\,\Bigg\{1-\frac{8\,\alpha^4}{\big[\alpha^2+(\boldsymbol{G}+\boldsymbol{k})^2\big]^2}\sum_{\boldsymbol{R}} e^{-\alpha|\boldsymbol{r}-\boldsymbol{R}|}\,e^{-i(\boldsymbol{G}+\boldsymbol{k})\cdot(\boldsymbol{r}-\boldsymbol{R})}\Bigg\} \quad . \tag{1.118}$$

For $\boldsymbol{G}+\boldsymbol{k}=0$, we have, in the $\boldsymbol{R}=0$ cell,

$$\phi_0(\boldsymbol{r}) \approx \frac{1}{\sqrt{V}}\big(1-8\,e^{-\alpha r}\big) \quad . \tag{1.119}$$

Note that the OPW states are not normalized. Indeed, we have[20]

$$\langle\,\phi_{\boldsymbol{G}+\boldsymbol{k}}\,|\,\phi_{\boldsymbol{G}+\boldsymbol{k}}\,\rangle = \int\! d^d r\,\big|\phi_{\boldsymbol{G}+\boldsymbol{k}}(\boldsymbol{r})\big|^2 = 1-\frac{1}{V}\sum_{\mathsf{a}}\bigg|\int\! d^d r\,u_{\mathsf{a}\boldsymbol{k}}(\boldsymbol{r})\,e^{-i\boldsymbol{G}\cdot\boldsymbol{r}'}\bigg|^2 \quad . \tag{1.120}$$

The energy eigenvalues are then obtained by solving the equation $\det\,M_{\boldsymbol{G}\boldsymbol{G}'}(\boldsymbol{k},E)=0$ for $E_n(\boldsymbol{k})$, where

$$\begin{aligned} M_{\boldsymbol{G}\boldsymbol{G}'}(\boldsymbol{k},E) &= \langle\,\phi_{\boldsymbol{G}+\boldsymbol{k}}\,|\,H\,|\,\phi_{\boldsymbol{G}'+\boldsymbol{k}}\,\rangle \\ &= \bigg[\frac{\hbar^2(\boldsymbol{G}+\boldsymbol{k})^2}{2m}-E\bigg]\delta_{\boldsymbol{G}\boldsymbol{G}'}+V_{\boldsymbol{G}-\boldsymbol{G}'}+\sum_{\mathsf{a}}\big[E-E_{\mathsf{a}}(\boldsymbol{k})\big]\,\langle\,\boldsymbol{G}+\boldsymbol{k}\,|\,\mathsf{a}\boldsymbol{k}\,\rangle\,\langle\,\mathsf{a}\boldsymbol{k}\,|\,\boldsymbol{G}'+\boldsymbol{k}\,\rangle \ . \end{aligned} \tag{1.121}$$

The overlap of the plane wave state $|\,\boldsymbol{G}+\boldsymbol{k}\,\rangle$ and the core Bloch state $|\,\mathsf{a}\boldsymbol{k}\,\rangle$ is given by

$$\langle\,\boldsymbol{G}+\boldsymbol{k}\,|\,\mathsf{a}\boldsymbol{k}\,\rangle = N^{1/2}\,v_0^{-1/2}\int\limits_{\Omega} d^d r\,u_{\mathsf{a}\boldsymbol{k}}(\boldsymbol{r})\,e^{-i\boldsymbol{G}\cdot\boldsymbol{r}} \quad . \tag{1.122}$$

---

[20] Note that $0 \le \langle\,\phi_{\boldsymbol{k}}\,|\,\phi_{\boldsymbol{k}}\,\rangle \le 1$.

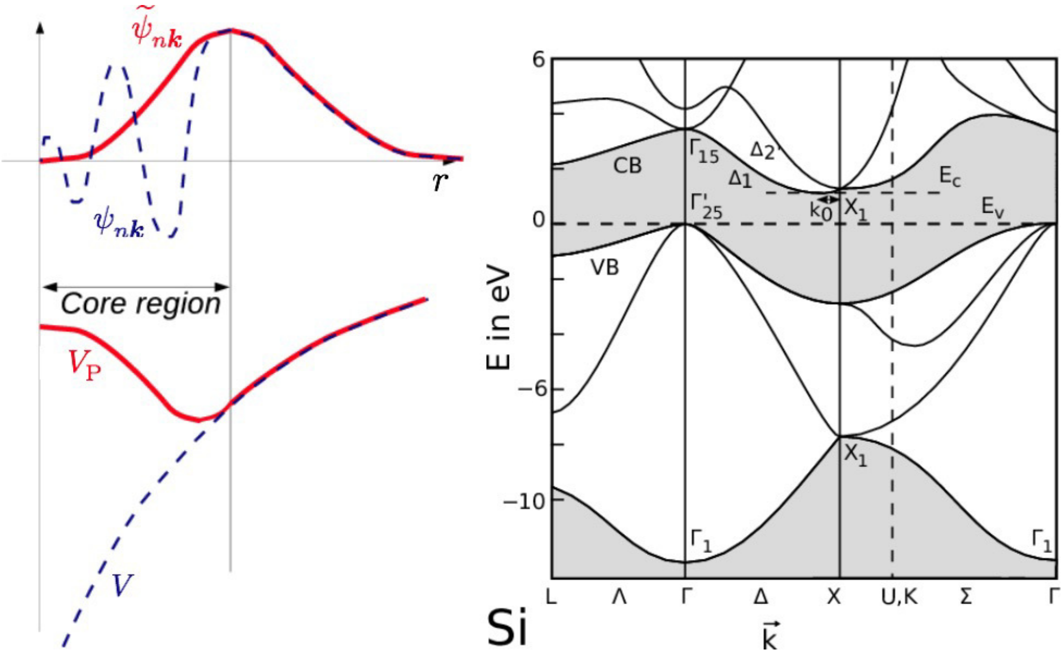

Figure 1.15: Left: Blue curves sketch the potential V in the vicinity of a nucleus, and corresponding valence or conduction band wavefunction $\psi_{n\boldsymbol{k}}$. Note that $\psi_{n\boldsymbol{k}}$ wiggles significantly in the vicinity of the nucleus because it must be orthogonal to the core atomic orbitals. Red curves sketch the pseudopotential $V_{\rm P}$ and corresponding pseudo-wavefunction $\widetilde{\psi}_{n\boldsymbol{k}}$. Right: pseudopotential calculation for the band structure of Si.

1.5.2 The pseudopotential

Equivalently, we may use the $|\,\phi_{\boldsymbol{G}+\boldsymbol{k}}\,\rangle$ in linear combinations to build our Bloch states, *viz.*

$$|\,\psi_{n\boldsymbol{k}}\,\rangle = \sum_{\boldsymbol{G}} C^{(n)}_{\boldsymbol{G}}(\boldsymbol{k})\,|\,\phi_{\boldsymbol{G}+\boldsymbol{k}}\,\rangle \equiv (1-\Pi)\,|\,\widetilde{\psi}_{n\boldsymbol{k}}\,\rangle \quad , \tag{1.123}$$

where $|\,\widetilde{\psi}_{n\boldsymbol{k}}\,\rangle = \sum_{\boldsymbol{G}} C^{(n)}_{\boldsymbol{G}}(\boldsymbol{k})\,|\,\boldsymbol{G}+\boldsymbol{k}\,\rangle$. Note that the *pseudo-wavefunction* $\widetilde{\psi}_{n\boldsymbol{k}}(\boldsymbol{r})$ is a sum over plane waves. What equation does it satisfy? From $H|\,\psi_{n\boldsymbol{k}}\,\rangle = E\,|\,\psi_{n\boldsymbol{k}}\,\rangle$, we derive

$$H|\,\widetilde{\psi}_{n\boldsymbol{k}}\,\rangle + \overbrace{(E-H)\,\Pi}^{V_{\rm R}}\,|\,\widetilde{\psi}_{n\boldsymbol{k}}\,\rangle = E\,|\,\widetilde{\psi}_{n\boldsymbol{k}}\,\rangle \quad . \tag{1.124}$$

Note that

$$V_{\rm R} = (E-H)\,\Pi = \sum_{\mathsf{a}} \big[E - E_{\mathsf{a}}(\boldsymbol{k})\big]\,|\,\mathsf{a}\boldsymbol{k}\,\rangle\langle\,\mathsf{a}\boldsymbol{k}\,| \tag{1.125}$$

and

$$\langle\,\boldsymbol{r}\,|\,V_{\rm R}\,|\,\widetilde{\psi}\,\rangle = \int d^d r'\; V_{\rm R}(\boldsymbol{r},\boldsymbol{r}')\,\widetilde{\psi}(\boldsymbol{r}') \quad , \tag{1.126}$$

where

$$\begin{aligned} V_{\rm R}(\boldsymbol{r},\boldsymbol{r}') &= \sum_{\mathsf{a},\boldsymbol{k}} \big[E - E_{\mathsf{a}}(\boldsymbol{k})\big]\, \psi_{\mathsf{a}\boldsymbol{k}}(\boldsymbol{r})\, \psi^*_{\mathsf{a}\boldsymbol{k}}(\boldsymbol{r}') \\ &\approx \sum_{\mathsf{a},\boldsymbol{R}} (E - E_{\mathsf{a}}) \int d^d r'\; \varphi_{\mathsf{a}}(\boldsymbol{r}-\boldsymbol{R})\, \varphi^*_{\mathsf{a}}(\boldsymbol{r}'-\boldsymbol{R}) \quad , \end{aligned} \tag{1.127}$$

where $\varphi_{\mathsf{a}}(\boldsymbol{r})$ is the $\mathsf{a}^{\rm th}$ atomic core wavefunction. The approximation in the second line above is valid in the limit where the core energy bands are dispersionless, and $E_{\mathsf{a}}(\boldsymbol{k})$ is replaced by the $\boldsymbol{k}$-independent atomic eigenvalue E_{a}. We then use $\sum_{\boldsymbol{k}} |\, \mathsf{a}\boldsymbol{k}\,\rangle\langle\, \mathsf{a}\boldsymbol{k}\,| = \sum_{\boldsymbol{R}} |\, \mathsf{a}\boldsymbol{R}\,\rangle\langle\, \mathsf{a}\boldsymbol{R}\,|$, with $\langle\, \boldsymbol{r}\,|\, \mathsf{a}\boldsymbol{R}\,\rangle \approx \varphi_{\mathsf{a}}(\boldsymbol{r}-\boldsymbol{R})$. Because the atomic levels are highly localized, this means $V_{\boldsymbol{R}}(\boldsymbol{r},\boldsymbol{r}')$ is very small unless both $\boldsymbol{r}$ and $\boldsymbol{r}'$ lie within the same core region. Thus, $V_{\rm R}(\boldsymbol{r},\boldsymbol{r}')$ is "almost diagonal" in $\boldsymbol{r}$ and $\boldsymbol{r}'$. Since the energies of interest satisfy $E > E_{\mathsf{a}}$, the term $V_{\boldsymbol{R}}$ tends to add to what is a negative (attractive) potential V, and the combination $V_{\rm P} = V + V_{\rm R}$, known as the *pseudopotential*, is in general weaker the original potential. As depicted in the left panel of Fig. 1.15, whereas the actual valence or conduction band Bloch states $\psi_{{\rm c/v},\boldsymbol{k}}(\boldsymbol{r})$ must wiggle rapidly in the vicinity of each nucleus, in order to be orthogonal to the atomic core states and thereby necessitating the contribution of a large number of high wavevector plane wave components, each pseudo-wavefunction $\widetilde{\psi}_{n\boldsymbol{k}}(\boldsymbol{r})$ is unremarkable in the core region, and can be described using far less information.

In fact, there is a great arbitrariness in defining the operator $V_{\rm R}$. Suppose we take $\widetilde{V}_{\rm R} = \Pi\, W$, where W is *any* operator. Note that

$$\widetilde{V}_{\rm R}(\boldsymbol{r},\boldsymbol{r}') = \langle\, \boldsymbol{r}\,|\, \Pi\, W\,|\, \boldsymbol{r}'\,\rangle = \sum_{\mathsf{a},\boldsymbol{k}} \psi_{\mathsf{a}\boldsymbol{k}}(\boldsymbol{r})\, \langle\, \mathsf{a}\boldsymbol{k}\,|\, W\,|\, \boldsymbol{r}'\,\rangle \equiv \sum_{\mathsf{a},\boldsymbol{k}} \psi_{\mathsf{a}\boldsymbol{k}}(\boldsymbol{r})\, A^*_{\mathsf{a}\boldsymbol{k}}(\boldsymbol{r}') \quad . \tag{1.128}$$

This needn't even be Hermitian! The point is that $H = T + V$ and $\widetilde{H} = T + V + \widetilde{V}_{\rm R}$ have the same eigenvalues so long as they are acting outside the space of core wavefunctions. To see this, let us suppose

$$H\,|\,\psi\,\rangle = E\,|\,\psi\,\rangle \qquad , \qquad \widetilde{H}\,|\,\xi\,\rangle = \widetilde{E}\,|\,\xi\,\rangle \quad . \tag{1.129}$$

Then

$$\begin{aligned} \widetilde{E}\,\langle\,\psi\,|\,\xi\,\rangle = \langle\,\psi\,|\,\widetilde{H}\,|\,\xi\,\rangle &= \langle\,\psi\,|\,(H + \Pi\, W)\,|\,\xi\,\rangle \\ &= E\,\langle\,\psi\,|\,\xi\,\rangle + \langle\,\psi\,|\,\Pi\, W\,|\,\xi\,\rangle \quad . \end{aligned} \tag{1.130}$$

Now if $|\,\psi\,\rangle$ lies in the complement of that part of the Hilbert space spanned by the core states, then $\Pi\,|\,\psi\,\rangle = 0$, and it follows that $(E - \widetilde{E})\,\langle\,\psi\,|\,\xi\,\rangle = 0$, hence $E = \widetilde{E}$, so long as $\langle\,\psi\,|\,\xi\,\rangle \neq 0$. If we want $V_{\rm P}$ to be Hermitian, a natural choice might be $\widetilde{V}_{\rm R} = -\Pi\, V\, \Pi$, which gives $V_{\rm P} = V - \Pi\, V\, \Pi$. This effectively removes from the potential V any component which can be constructed from core states alone.

1.6 Semiclassical Dynamics of Bloch Electrons

Consider a time-evolving quantum mechanical state $|\psi(t)\rangle$. The time dependence of the expectation value $\mathcal{O}(t) = \langle\psi(t)|\mathcal{O}|\psi(t)\rangle$ satisfies

$$\frac{d\mathcal{O}}{dt} = \frac{i}{\hbar}\,\langle\,\psi(t)\,|\,[H,\mathcal{O}]\,|\,\psi(t)\,\rangle \quad . \tag{1.131}$$

Thus for $H = \frac{\boldsymbol{p}^2}{2m} + V(\boldsymbol{r})$ we have $\frac{d}{dt}\langle\boldsymbol{r}\rangle = \langle\frac{\boldsymbol{p}}{m}\rangle$ and $\frac{d}{dt}\langle\boldsymbol{p}\rangle = -\langle\boldsymbol{\nabla}V\rangle$, a result known as Ehrenfest's theorem. There are a couple of problems in applying this to electrons in crystals, though. One is that the momentum $\boldsymbol{p}$ in a Bloch state is defined only modulo $\hbar\boldsymbol{G}$, where $\boldsymbol{G}$ is any reciprocal lattice vector. Another is that the potential $\Delta V(\boldsymbol{r}) = e\boldsymbol{E}\cdot\boldsymbol{r}$ breaks the lattice periodicity present in the crystal.

1.6.1 Adiabatic evolution

Here we assume $d = 3$ dimensions. Recall $\boldsymbol{E} = -\boldsymbol{\nabla}\phi - c^{-1}\partial_t\boldsymbol{A}$, so rather that taking $\boldsymbol{A} = 0$ and $\phi = -\boldsymbol{E}\cdot\boldsymbol{r}$ in the case of a uniform electric field, we can instead take $\boldsymbol{A}(t) = -c\boldsymbol{E}t$ and $\phi = 0$ and write

$$H(t) = \frac{\big(\boldsymbol{p} + \frac{e}{c}\boldsymbol{A}(t)\big)^2}{2m} + V(\boldsymbol{r}) \quad , \tag{1.132}$$

with $\partial_t\boldsymbol{A} = -c\boldsymbol{E}$, and $\boldsymbol{\nabla}\times\boldsymbol{A} = \boldsymbol{B}$ if there is a magnetic field as well. We assume that the electric field is very weak, which means that we can treat the time dependent Hamiltonian $H(t)$ in the adiabatic limit[21].

Consider a setting in which a Hamiltonian $H(\boldsymbol{\lambda})$ depends on a set of parameters $\boldsymbol{\lambda} = \{\lambda_1, \ldots, \lambda_K\}$. The *adiabatic eigenstates* of $H(\boldsymbol{\lambda})$ are denoted as $|n(\boldsymbol{\lambda})\rangle$, where $H(\boldsymbol{\lambda})\,|n(\boldsymbol{\lambda})\rangle = E_n(\boldsymbol{\lambda})\,|n(\boldsymbol{\lambda})\rangle$. Now suppose that $\lambda(t)$ varies with time. Since the set $\big\{|n(\boldsymbol{\lambda})\rangle\big\}$ is complete, we may expand the wavefunction $|\psi(t)\rangle$ in the adiabatic basis, *viz.*

$$|\,\psi(t)\,\rangle = \sum_n a_n(t)\,|\,n\big(\boldsymbol{\lambda}(t)\big)\,\rangle \quad . \tag{1.133}$$

Now we impose the condition $i\hbar\,\partial_t\,|\psi(t)\rangle = H\big(\boldsymbol{\lambda}(t)\big)|\psi(t)\rangle$. We first define the phases $\phi_n(t)$ and $\gamma_n(t)$, where

$$\phi_n(t) = -\frac{1}{\hbar}\int^t\! dt'\, E_n\big(\boldsymbol{\lambda}(t')\big) \tag{1.134}$$

and where $\gamma_n(t)$ satisfies

$$\frac{d\gamma_n}{dt} = i\,\langle\, n\big(\boldsymbol{\lambda}(t)\big)\,|\,\frac{d}{dt}\,|\,n\big(\boldsymbol{\lambda}(t)\big)\,\rangle \quad . \tag{1.135}$$

Then, writing $a_n(t) \equiv e^{i\phi_n(t)}\,e^{i\gamma_n(t)}\,\alpha_n(t)$, we find

$$\frac{d\alpha_n}{dt} = -{\sum_l}' e^{i(\gamma_l-\gamma_n)}\,e^{i(\phi_l-\phi_n)}\,\alpha_l \quad , \tag{1.136}$$

where the prime on the sum indicates that the term $l = n$ is to be excluded. Now consider initial conditions where $a_l(0) = \delta_{ln}$. Since the evolution is adiabatic, the phases $\phi_l(t)$ are the fastest evolving quantities, with $\partial_t\,\phi_l = -E_l/\hbar = \mathcal{O}(1)$, as opposed to γ_l and α_l, which vary on the slow time scale associated with the evolution of $\boldsymbol{\lambda}(t)$. This allows us to approximately integrate the above equations to obtain

$$\alpha_n(t) \approx \alpha_n(0) = 1 \qquad , \qquad \alpha_l(t) \approx -i\hbar\,\frac{\langle\, l\,|\,\partial_t\,|\,n\,\rangle}{E_l - E_n} \quad . \tag{1.137}$$

Thus,

$$|\,\psi(t)\,\rangle \approx e^{i\phi_n(t)}\,e^{i\gamma_n(t)}\left\{|\,n(t)\,\rangle - i\hbar{\sum_l}'\frac{|\,l(t)\,\rangle\langle\, l(t)\,|\,d_t\,|\,n(t)\,\rangle}{E_l(t) - E_n(t)}\right\} \quad , \tag{1.138}$$

---

[21] Technically, we should require there be a finite energy gap in order to justify adiabatic evolution.

where each $|\, l(t)\,\rangle = |\, l\big(\boldsymbol{\lambda}(t)\big)\,\rangle$, and where $d_t = d/dt$ is the total time derivative. Note that we can write

$$\frac{d\,|n\rangle}{dt} = \frac{\partial\,|n\rangle}{\partial\lambda_\mu} \cdot \frac{d\lambda_\mu}{dt} \quad , \tag{1.139}$$

with an implied sum on μ, and with $i\,\langle n|d_t|n\rangle = \mathcal{A}^\mu_n\,\dot{\lambda}_\mu$, where

$$\mathcal{A}^\mu_n(\boldsymbol{\lambda}) \equiv i\,\langle\, n(\boldsymbol{\lambda})\,|\,\frac{\partial}{\partial\lambda_\mu}\,|\, n(\boldsymbol{\lambda})\,\rangle \tag{1.140}$$

is the *geometric connection* (or *Berry connection*) for the state $|\, n(\boldsymbol{\lambda})\,\rangle$. Note that the Berry connection is gauge-dependent, in that redefining $|\,\tilde{n}(\boldsymbol{\lambda})\,\rangle \equiv e^{if_n(\boldsymbol{\lambda})}\,|\, n(\boldsymbol{\lambda})\,\rangle$ results in

$$\widetilde{\mathcal{A}}^\mu_n(\boldsymbol{\lambda}) = i\,\langle\,\tilde{n}(\boldsymbol{\lambda})\,|\,\frac{\partial}{\partial\lambda_\mu}\,|\,\tilde{n}(\boldsymbol{\lambda})\,\rangle = \mathcal{A}^\mu_n(\boldsymbol{\lambda}) - \frac{\partial f_n}{\partial\lambda_\mu} \quad . \tag{1.141}$$

If we require that the adiabatic wavefunctions be single-valued as a function of $\boldsymbol{\lambda}$, then *the integral of the Berry connection around a closed path is a gauge-invariant quantity*,

$$\gamma_n(\mathcal{C}) \equiv \oint\limits_{\mathcal{C}} d\lambda_\mu\,\mathcal{A}^\mu_n(\boldsymbol{\lambda}) \quad , \tag{1.142}$$

since $f_n(\boldsymbol{\lambda})$ can wind only by $2\pi k$, with $k \in \mathbb{Z}$, around a closed loop $\mathcal{C}$ in parameter space. If $\mathcal{C}$ is contractable to a point, then $k = 0$.

Now consider the cell function $|u_{n\boldsymbol{k}}\rangle$ as a function of the Bloch wavevector $\boldsymbol{k}$ for each band index n. The velocity operator is $\boldsymbol{v}(k) = \hbar^{-1}\,\partial H(\boldsymbol{k})/\partial\boldsymbol{k}$, where $H(\boldsymbol{k}) = e^{-i\boldsymbol{k}\cdot\boldsymbol{r}} H e^{i\boldsymbol{k}\cdot\boldsymbol{r}}$. We then have

$$\begin{aligned} \frac{d\boldsymbol{r}}{dt} &= \langle\,\psi(t)\,|\,\boldsymbol{v}(\boldsymbol{k})\,|\,\psi(t)\,\rangle \\ &= \frac{1}{\hbar}\,\frac{\partial E_n(\boldsymbol{k})}{\partial\boldsymbol{k}} - \frac{d\boldsymbol{k}}{dt} \times \boldsymbol{\varOmega}_n(\boldsymbol{k}) \end{aligned} \tag{1.143}$$

where

$$\varOmega^\mu_n(\boldsymbol{k}) = \epsilon_{\mu\nu\lambda}\,\frac{\partial\mathcal{A}^\lambda_n(\boldsymbol{k})}{\partial k^\nu} \quad , \quad \mathcal{A}^\mu_n(\boldsymbol{k}) = i\,\Big\langle\, u_{n\boldsymbol{k}}\,\Big|\,\frac{\partial}{\partial k^\mu}\,\Big|\,u_{n\boldsymbol{k}}\,\Big\rangle \quad . \tag{1.144}$$

In vector notation, $\boldsymbol{\mathcal{A}}_n(\boldsymbol{k}) = i\,\langle\, u_{n\boldsymbol{k}}\,|\,\widetilde{\boldsymbol{\nabla}}\,|\,u_{n\boldsymbol{k}}\,\rangle$ and $\boldsymbol{\varOmega}_n(\boldsymbol{k}) = \widetilde{\boldsymbol{\nabla}} \times \boldsymbol{\mathcal{A}}_n(\boldsymbol{k})$, where $\widetilde{\boldsymbol{\nabla}} = \frac{\partial}{\partial\boldsymbol{k}}$. Eqn. 1.143 is the first of our semiclassical equations of motion for an electron wavepacket in a crystal. The quantity $\boldsymbol{\varOmega}_n(\boldsymbol{k})$, which has dimensions of area, is called the *Berry curvature* of the band $|u_{n\boldsymbol{k}}\rangle$. The second term in Eqn. 1.143 is incorrectly omitted in many standard solid state physics texts! When the orbital moment of the Bloch electrons is included, we must substitute[22]

$$E_n(\boldsymbol{k}) \to E_n(\boldsymbol{k}) - \boldsymbol{M}_n(\boldsymbol{k}) \cdot \boldsymbol{B}(\boldsymbol{r},t) \quad , \tag{1.145}$$

where

$$M^\mu_n(\boldsymbol{k}) = e\,\epsilon_{\mu\nu\lambda}\,\mathsf{Im}\,\left\langle \frac{\partial u_{n\boldsymbol{k}}}{\partial k^\nu}\,\middle|\,\big[E_n(\boldsymbol{k}) - H(\boldsymbol{k})\big]\,\middle|\,\frac{\partial u_{n\boldsymbol{k}}}{\partial k^\lambda}\right\rangle \quad , \tag{1.146}$$

---

[22] See G. Sundaram and Q. Niu, *Phys. Rev. B* **59**, 14915 (1999).

and $H(\boldsymbol{k}) = \frac{(\boldsymbol{p}+\hbar\boldsymbol{k})^2}{2m} + V(\boldsymbol{r})$ as before.

The second equation of semiclassical motion is for $d\boldsymbol{k}/dt$. This is the familiar equation derived from Newton's second law[23],

$$\frac{d\boldsymbol{k}}{dt} = -\frac{e}{\hbar}\,\boldsymbol{E} - \frac{e}{\hbar c}\,\frac{d\boldsymbol{r}}{dt} \times \boldsymbol{B} - \frac{e}{2\hbar mc}\,\boldsymbol{\nabla}(\boldsymbol{\sigma}\cdot\boldsymbol{B}) \quad , \tag{1.147}$$

where we have included the contribution from the spin-orbit Hamiltonian $H_{\textsf{so}} = -\frac{e}{2mc}\,\boldsymbol{\sigma}\cdot\boldsymbol{B}$.

1.6.2 Violation of Liouville's theorem and its resolution

Our equations of motion for a wavepacket are thus

$$\begin{aligned} \dot{x}^\alpha + \epsilon_{\alpha\beta\gamma}\,\dot{k}^\beta\,\Omega^\gamma_n &= v^\alpha_n \\ \dot{k}^\alpha + \frac{e}{\hbar c}\,\epsilon_{\alpha\beta\gamma}\,\dot{x}^\beta B^\gamma &= -\frac{e}{\hbar}\,E^\alpha \quad , \end{aligned} \tag{1.148}$$

where $\boldsymbol{v}_n(\boldsymbol{k}) = \widetilde{\boldsymbol{\nabla}} E_n(\boldsymbol{k})/\hbar$. These equations may be recast as

$$\begin{pmatrix} \delta_{\alpha\beta} & \epsilon_{\alpha\beta\gamma}\,\Omega^\gamma_n \\ \frac{e}{\hbar c}\,\epsilon_{\alpha\beta\gamma}\,B^\gamma & \delta_{\alpha\beta} \end{pmatrix} \begin{pmatrix} \dot{x}^\alpha \\ \dot{k}^\alpha \end{pmatrix} = \begin{pmatrix} v^\alpha_n \\ -\frac{e}{\hbar}\,E^\alpha \end{pmatrix} \quad . \tag{1.149}$$

Inverting, we find

$$\begin{aligned} \dot{x}^\alpha &= \big(1 + \tfrac{e}{\hbar c}\boldsymbol{B}\cdot\boldsymbol{\Omega}_n\big)^{-1}\Big\{ v^\alpha_n + \tfrac{e}{\hbar c}\,(\boldsymbol{v}_n\cdot\boldsymbol{\Omega}_n)\,B^\alpha + \tfrac{e}{\hbar}\,\epsilon_{\alpha\beta\gamma}\,E^\beta\,\Omega^\gamma_n \Big\} \\ \dot{k}^\alpha &= -\tfrac{e}{\hbar}\,\big(1 + \tfrac{e}{\hbar c}\boldsymbol{B}\cdot\boldsymbol{\Omega}_n\big)^{-1}\Big\{ E^\alpha + \tfrac{e}{\hbar c}\,(\boldsymbol{E}\cdot\boldsymbol{B})\,\Omega^\alpha_n + \tfrac{1}{c}\,\epsilon_{\alpha\beta\gamma}\,v^\beta\,B^\gamma \Big\} \quad . \end{aligned} \tag{1.150}$$

It is straightforward to derive the result

$$\frac{\partial \dot{x}^\alpha}{\partial x^\alpha} + \frac{\partial \dot{k}^\alpha}{\partial k^\alpha} = -\frac{\partial \ln D_n}{\partial x^\alpha}\,\frac{dx^\alpha}{dt} - \frac{\partial \ln D_n}{\partial k^\alpha}\,\frac{dk^\alpha}{dt} - \frac{\partial \ln D}{\partial t} = -\frac{d\ln D_n}{dt} \quad , \tag{1.151}$$

where

$$D_n(\boldsymbol{r},\boldsymbol{k},t) = 1 + \frac{e}{\hbar c}\,\boldsymbol{B}(\boldsymbol{r},t)\cdot\boldsymbol{\Omega}_n(\boldsymbol{k}) \tag{1.152}$$

is dimensionless. As discussed by Xiao, Shi, and Niu[24], this implies a violation of Liouville's theorem, as phase space volumes will then expand according to $d\ln\Delta V/dt = \boldsymbol{\nabla}_{\boldsymbol{r}}\cdot\dot{\boldsymbol{r}} + \boldsymbol{\nabla}_{\boldsymbol{k}}\cdot\dot{\boldsymbol{k}} = -d\ln D_n(\boldsymbol{r},\boldsymbol{k},t)/dt$, where $\Delta V = \Delta\boldsymbol{r}\,\Delta\boldsymbol{k}$ is a phase space volume element. Thus, $\Delta V(t) = \Delta V(0)/D_n(\boldsymbol{r},\boldsymbol{k},t)$, and this inconvenience can be eliminated by defining the phase space probability density as

$$\rho_n(\boldsymbol{r},\boldsymbol{k},t) = D_n(\boldsymbol{r},\boldsymbol{k},t)\,f_n(\boldsymbol{r},\boldsymbol{k},t) \quad , \tag{1.153}$$

---

[23] Some subtleties in the derivation are discussed in A. Manohar, *Phys. Rev. B* **34**, 1287 (1986).

[24] See D. Xiao, J. Shi, and Q. Niu, *Phys. Rev. Lett.*. **95**, 137204 (2005).

where $f_n(\boldsymbol{r},\boldsymbol{k},t)$ is the occupation number of the state $|\,n\boldsymbol{k}\,\rangle$ in the region centered at $\boldsymbol{r}$. For homogeneous systems, this means that the expectation of any observable $\mathcal{O}$ is given by

$$\langle\mathcal{O}\rangle = \sum_n \int\limits_{\hat{\Omega}} \frac{d^3k}{(2\pi)^3}\, D_n(\boldsymbol{k})\, f_n(\boldsymbol{k})\, \langle\, u_{n\boldsymbol{k}}\,|\,\mathcal{O}\,|\,u_{n\boldsymbol{k}}\,\rangle \quad , \tag{1.154}$$

where, in equilibrium, $f_n(\boldsymbol{k})$ is the Fermi function $f\big(E_n(\boldsymbol{k})-\mu\big)$. The electrical current density carried by a given band n is then

$$\begin{aligned} j_n^\alpha &= \int\limits_{\hat{\Omega}} \frac{d^dk}{(2\pi)^d}\, \rho_n(\boldsymbol{k})\,(-e\dot{x}) \\ &= -e\int\limits_{\hat{\Omega}} \frac{d^3k}{(2\pi)^3} \bigg\{ v_n^\alpha + \frac{e}{\hbar c}\,(\boldsymbol{v}_n\cdot\boldsymbol{\Omega}_n)\,B^\alpha + \frac{e}{\hbar}\,\epsilon_{\alpha\beta\gamma}\,E^\beta\,\Omega_n^\gamma \bigg\}\, f_n(\boldsymbol{k}) \quad . \end{aligned} \tag{1.155}$$

Note the cancellation of the $D_n(\boldsymbol{k})$ factors in $\rho_n(\boldsymbol{k})$ and $\dot{x}$. Consider the case of a filled band, with $\boldsymbol{B}=0$. The total current density is then

$$\boldsymbol{j}_n = -\frac{e^2}{\hbar}\,\boldsymbol{E}\times\int\limits_{\hat{\Omega}} \frac{d^3k}{(2\pi)^3}\,\boldsymbol{\Omega}_n(\boldsymbol{k}) \quad . \tag{1.156}$$

1.6.3 Bloch oscillations

Let's consider the simplest context for our semiclassical equations of motion: $d=1$ dimension, which means $\boldsymbol{B}=0$. We'll take a nearest neighbor s orbital hopping Hamiltonian, whose sole tight binding band has the dispersion[25] $E(k)=-2\beta\cos(ka)$. The semiclassical equations of motion are

$$\dot{x} = \frac{1}{\hbar}\frac{\partial E}{\partial k} = \frac{2\beta a}{\hbar}\,\sin(ka) \qquad , \qquad \dot{k} = -\frac{e}{\hbar}\,E \quad . \tag{1.157}$$

The second of these equations is easily integrated for constant E:

$$k(t) = k(0) - \frac{e}{\hbar}Et \quad , \tag{1.158}$$

in which case

$$\dot{x} = \frac{2\beta a}{\hbar}\,\sin\!\Big(k(0)\,a - \frac{eaEt}{\hbar}\Big) \qquad \Rightarrow \qquad x(t) = x(0) + \frac{2\beta}{eE}\left[\cos\!\Big(k(0)\,a - \frac{eaEt}{\hbar}\Big) - \cos\!\big(k(0)\,a\big)\right] \quad . \tag{1.159}$$

Note that $x(t)$ oscillates in time! This is quite unlike the free electron case, where we have $m\ddot{x}=-eE$, yielding ballistic motion $x(t)=x(0)+\dot{x}(0)\,t-\frac{eE}{2m}\,t^2$, *i.e.* uniform acceleration $(-eE/m)$. This remarkable behavior is called a *Bloch oscillation*.

The period of the Bloch oscillations is $\tau_{\text{B}}=\hbar/eaE$. Let's estimate τ_{B}, taking $E=1\,\text{V/cm}$ and $a=3\,\text{Å}$. We find $\tau_{\text{B}}=1.4\times10^{-7}\,\text{s}$, which is much larger than typical scattering times due to phonons or lattice impurities. For example, the thermal de Broglie lifetime is $\hbar/k_{\text{B}}T=2.5\times10^{-14}\,\text{s}$ at $T=300\,\text{K}$. Thus, the wavepacket never makes it across the Brillouin zone - not even close. In the next chapter, we will see how to model charge transport in metals.

---

[25] We write the hopping integral as β so as to avoid any confusion with the time variable, t.